ChemPubSoc Europe

DOI: 10.1002/chem.201xxxxxx

CHEMISTRY
A European Journal
Full Paper

Fluorescence

D-π-A Triarylboron Compounds with Tunable Push-Pull Character Achieved by Modification of Both the Donor and Acceptor Moieties

Zuolun Zhang,[a] Robert M. Edkins,[a] Jörn Nitsch,[a] Katharina Fucke,[a, b] Antonius Eichhorn,[a] Andreas Steffen,[a] Yue Wang,[c] and Todd B. Marder*[a]

Abstract: The push-pull character of a series of donor-bithienyl-acceptor compounds has been tuned by adopting triphenylamine or 1,1,7,7-tetramethyljulolidine as a donor and B(2,6-Me_2-4-R-C_6H_2)$_2$ (R = Me, C_6F_5 or 3,5-$(CF_3)_2$-C_6H_3) or B(2,4,6-$(CF_3)_3$-C_6H_2)$_2$ as an acceptor. Ir-catalyzed C–H borylation was utilized in the derivatization of the boryl acceptors and the tetramethyljulolidine donor. The donor and acceptor strengths were evaluated by electrochemical and photophysical measurements. In solution, the compound with the strongest acceptor, B(2,4,6-$(CF_3)_3$-C_6H_2)$_2$ ($(FMes)_2B$), has strongly quenched emission, while all other compounds show efficient green to red (Φ_F 0.80–1.00) or NIR (Φ_F 0.27–0.48) emission, depending on solvent. Notably, this study presents the first examples of efficient NIR emission from three-coordinate boron compounds. Efficient solid-state red emission was observed for some derivatives, and interesting aggregation-induced emission of the $(FMes)_2B$-containing compound was studied. Moreover, each compound showed a strong and clearly visible response to fluoride addition, with either a large emission-color change or turn-on fluorescence.

Introduction

Three-coordinate organoboron compounds are an important class of materials for optical and optoelectronic applications.[1-7] In particular, donor-(π-spacer)-acceptor (D-π-A) organoboron systems with an aromatic amine donor group and a boryl acceptor group have attracted tremendous research interest.[8-11] Such push-pull systems usually show strong intramolecular charge-transfer (ICT) emission, which make them promising materials for applications in nonlinear optics (NLO),[9] organic light-emitting diodes (OLEDs),[10] and anion sensing.[11] Modification of each of the donor, π-spacer, or acceptor groups has been shown to be effective for tuning the properties of the materials.[8-11] Considering the 'push-pull' structure and the ICT character of the excited states of these D-π-A compounds, the incorporation of strong donor and/or acceptor groups is important for improving some of the properties of this type of boron compounds: 1) higher HOMO and lower LUMO energies arising from stronger donors and acceptors, respectively, can enhance the carrier-injecting properties of the materials in OLEDs,[12] which may improve device performance; 2) smaller HOMO-LUMO gaps may lead to red/near-infrared (NIR) emissive materials, which are rare for three-coordinate boron-based systems, particularly in the solid state;[3i,j,13] 3) red-shifted emission, caused by a stronger acceptor, may increase the difference in emission color before and after fluoride or cyanide coordination to the boron center and, thus, facilitate naked-eye detection of these important analytes.[4c] Therefore, we were motivated to develop organoboron compounds with strong push-pull character by strengthening the acceptor and/or donor groups. Up until now, many different donors have been employed in this type of compound;[8-11] however, the boryl acceptor is still quite limited, with the group bis(mesityl)boryl ($(Mes)_2B$) typically used, in which the sterically bulky mesityl substituents decrease the reactivity of the boron center towards nucleophiles, providing air stability. Although a few attempts to tune the boryl acceptors have been reported,[14] most of the modified boryl groups do not provide sufficient air-stability for the boron compounds, due to a lack of steric protection of the boron center.[4b,14a-d]

Recently, we introduced the strongly electron-accepting bis(fluoromesityl)boryl ($(FMes)_2B$) group into D-π-A systems.[15] In the present study, we modified the Mes_2B group through substitution of the methyl substituents *para* to the boron atom by electron-withdrawing perfluorophenyl and 3,5-bis(trifluoromethyl)phenyl substituents, to produce the acceptor groups $(Pfp)_2B$ and $(Tfp)_2B$, respectively (Scheme 1). To allow comparison of the acceptor strength of the known Mes_2B and $(FMes)_2B$ groups with the newly obtained $(Pfp)_2B$ and $(Tfp)_2B$

[a] *Dr. Z. Zhang, Dr. R. M. Edkins, J. Nitsch, Dr. K. Fucke, A. Eichhorn, Dr. A. Steffen, Prof. Dr. T. B. Marder*
Institut für Anorganische Chemie
Julius-Maximilians-Universität Würzburg
Am Hubland, 97074 Würzburg, Germany
Email: todd.marder@uni-wuerzburg.de

[b] *Dr. K. Fucke*
School of Medicine, Pharmacy and Health
Durham University
University Boulevard, Stockton-on-Tees, TS17 6BH, UK

[c] *Prof. Dr. Y. Wang*
State Key Laboratory of Supramolecular Structure and Materials
College of Chemistry, Jilin University
Changchun 130012, PR China

Supporting information for this article is available on the WWW under http://www.chemeurj.org/ or from the author.

groups, as well as to systematically study their influence on material properties, compounds **1**–**4** with the same triphenylamine (Tpa) donor group and each of these acceptors have been synthesized. Furthermore, to elucidate the influence of enhanced push-pull character, **5** and **6** have been prepared, which are analogues of **2** and **3** with a stronger 1,1,7,7-tetramethyljulolidine (Tmjul) donor group in conjunction with the $(Pfp)_2B$ and $(Tfp)_2B$ acceptor groups. In all of these compounds, 5,5′-substituted 2,2′-bithienyl was chosen as the π-spacer, because its electron-rich character and often close-to-coplanar structure were expected to facilitate long-wavelength emission.[16]

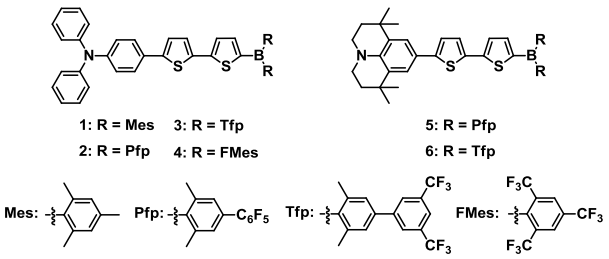

Scheme 1. Molecular structures of **1**–**6**.

Results and Discussion

Synthesis

The procedures used to synthesize compounds **1**–**6** are summarized in Scheme 2. **1**–**6** were obtained by reactions between the appropriate Tpa/Tmjul–bithienyl–Li and R_2BF precursors in an adaption of the typical method for synthesizing three-coordinate organoboron compounds.[4] The Tpa/Tmjul–bithienyl–Li reagents were prepared by lithiation of the products of the Suzuki-Miyaura cross-coupling reactions of Tpa–Br with [(2,2'-bithiophene)-5-yl]boronic acid or Tmjul-Bpin with 5-iodo-2,2'-bithiophene. The Tmjul–Bpin was obtained in high yield (88%) by regioselective iridium-catalyzed C–H borylation[17] of Tmjul–H on a multi-gram scale in hexane with a simple workup of filtration followed by washing with cold solvents (the crystal structure is shown in Figure S1). The C–H borylation of Tmjul-H is sterically controlled and, consequently, highly selective, leading to exclusive borylation at the 9-position, *i.e*. *para* to the nitrogen atom. This provides a facile and rapid route to the complementary nucleophilic coupling partner to 9-bromojulolidine, a compound that is widely used in the construction of D-π-A chromophores.[18] Furthermore, we note that simple adaption of the method might also be expected to expedite the synthesis of related Bpin-substituted planarized triphenylamines[19] and 2,6-substituted anilines[20] of pharmaceutical relevance, both of which otherwise require a two-step procedure of bromination and Pd-catalyzed Miyaura borylation. Key precursors Br–Pfp and Br–Tfp, required for modifying the boryl moiety, were prepared by Ir-catalyzed C–H borylation of 2,6-dimethylbromobenzene at the 4-position in 95% yield on a multi-gram scale, and subsequent Suzuki-Miyaura cross coupling with pentafluoroiodobenzene or 3,5-bis(trifluoromethyl)iodobenzene in 79–80% yield; notably, the borylation reaction was regiospecific and was, therefore, pivotal to ensuring high isolated yields of the products. The Grignard reagents prepared from these two precursors were reacted with BF_3•OEt_2 to produce the R_2BF precursors for the synthesis of **2**, **3**, **5** and **6**. These compounds were characterized by multinuclear NMR spectroscopy, mass spectrometry, and elemental analysis. The room temperature $^{19}F\{^1H\}$ NMR spectrum of **4** shows three broad peaks at –50.4, –52.1 and –56.5 ppm (1:1:2) for the four CF_3 groups of the FMes moieties that are in positions *ortho* to the boron atom and one singlet at –63.4 ppm for the two CF_3 groups at the *para*-positions (Figure S4), which indicates restricted rotation of the boron-bonded aryl rings. A similar phenomenon has been observed in our studies of $Ar–B(FMes)_2$ compounds.[15] At 223 K, the signals for the six CF_3 groups are fully separated, resulting in four quartets (two pairs, J = 11 and 13 Hz, respectively) and two singlets for the *ortho*- and *para*-CF_3 groups, respectively (Figure S4). This is different from the behavior of $Tpa–B(FMes)_2$,[15] which only displays two quartets and one singlet at 223 K for the *ortho*- and *para*-CF_3 groups, respectively. The loss of the C_2 symmetry along the B–C(thienyl) bond in compound **4**, accompanied by restricted rotation, is responsible for the complete inequality of the six CF_3 groups at low temperature, and the observed splitting of the signals into quartets for the *ortho*-CF_3 groups is due to through-space $^{19}F–^{19}F$ coupling.[15]

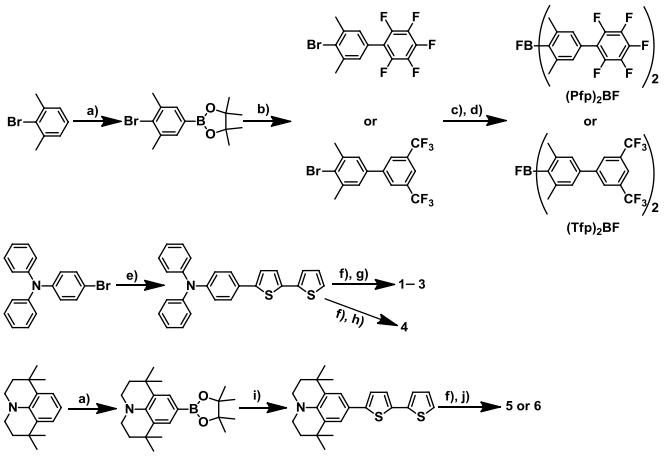

Scheme 2. Syntheses of compounds **1**–**6**. a) B_2pin_2, $[Ir(\mu\text{-}OMe)(COD)]_2$, 4,4′-di-*tert*-butyl-2,2′-bipyridine (dtbpy), hexane, 80 °C; b) C_6F_5I or $3,5\text{-}(CF_3)_2\text{-}C_6H_3\text{-}I$, Ag_2CO_3, $[Pd(PPh_3)_4]$, THF, reflux; c) Mg, $C_2H_4Br_2$, THF, r.t. to 60 °C; d) BF_3•OEt_2, 0 °C to 60 °C; e) [(2,2'-bithiophene)-5-yl]boronic acid, $[Pd(PPh_3)_4]$, Na_2CO_3, THF, H_2O, reflux; f) *n*-BuLi, THF, –78 °C; g) $(Mes)_2BF$/$(Tfp)_2BF$, –78 °C to r.t. or $(Pfp)_2BF$, 0 °C to r.t.; h) $(FMes)_2BF$, toluene, –25 °C to r.t.; i) 5-iodo-2,2'-bithiophene, Ag_2CO_3, $[Pd(PPh_3)_4]$, THF, reflux; j) $(Pfp)_2BF$, –78 °C to r.t. or $(Tfp)_2BF$, 0 °C to r.t..

Crystal Structures

To confirm the molecular structures and to investigate the influence of different donors and acceptors on the molecular conformations, single crystals of these compounds were grown and their structures were determined by X-ray diffraction. Single crystals of **2** were obtained by cooling the seeded melt and those of **4** were grown by crystallization from hexane solution at –30 °C. The crystal structures are shown in Figure 1, and selected bond lengths and dihedral angles are given in Table 1. The boron

atoms in both structures have a nearly perfect trigonal planar configuration, with the sum of the three C–B–C angles close to 360°. In **4**, the B1–C1 (1.605(4) Å) and B1–C9 (1.601(4) Å) bonds in the boryl group are significantly longer than the B1–C17 bond (1.518(4) Å), while the corresponding differences between the two types of B–C bonds in **2** are smaller (*ca.* 0.03–0.05Å). It has been observed previously that replacement of $(Mes)_2B$, for example, by more electron-withdrawing boryl groups, such as $(C_6F_5)_2B$[14a,b] and $(FMes)_2B$,[15] leads to an increase in such bond-length differences. Therefore, the large bond-length difference in **4** reflects the stronger acceptor strength of $(FMes)_2B$ than $(Pfp)_2B$. In **2**, the dihedral angles between the BC_3 plane and the 2,4,6-trisubstituted phenyl rings (P1 and P2) are similar to each other (59.9(3) and 57.8(2)°) and to the analogous dihedral angles (*ca.* 57–59°) in the compound 4-Me_2N–C_6H_4–CH=CH–2′,5′-thienyl–$B(Mes)_2$,[9p] while the related dihedral angles in **4** show a large difference (67.5(2) and 43.9(2)°). The dihedral angles between the two thienyl rings (T1 and T2) are 19.0(2) and 12.7(2)° in **2** and **4**, respectively, allowing good conjugation. The dithienyl π-system is also relatively planar with respect to the adjacent BC_3 plane and the diphenylamine-substituted phenyl ring (P3), exhibiting dihedral angles of 15.8(2) in **2** and 19.1(2)° in **4** between T1 and the BC_3 plane and 25.5(2) in **2** and 18.6(1)° in **4** between T2 and P3. In compound **2**, the two C_6F_5 groups (P4 and P5) and the adjacent phenyl rings (P1 and P2, respectively) exhibit dihedral angles of 51.6(3) and 61.8(2)° and are, thus, expected to be relatively poorly conjugated in the solid-state.

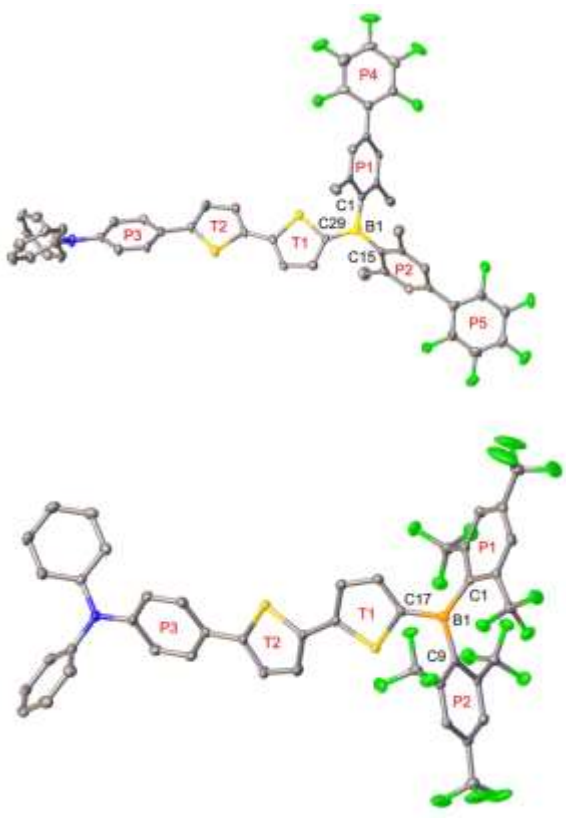

Figure 1. Molecular structures of **2** (top) and **4** (bottom) from single-crystal X-ray diffraction. Hydrogen atoms are omitted for clarity. The phenyl rings related to the discussion are labeled P1–P5, and the thienyl rings are labeled T1 and T2. Element (color): carbon (gray), nitrogen (blue), sulfur (yellow), boron (orange) and fluorine (green).

Table 1. Selected bond lengths (Å) and dihedral angles (°) for **2** and **4**, as obtained by single-crystal X-ray diffraction.

	2	**4**
B1–C1	1.584(9)	1.605(4)
B1-C15/B1–C9	1.565(9)	1.601(4)
B1-C29/B1–C17	1.532(9)	1.518(4)
∠P1–BC3 plane	59.9(3)	67.5(2)
∠P2–BC3 plane	57.8(2)	43.9(2)
∠T1–BC3 plane	15.8(2)	19.1(2)
∠T1–T2	19.0(2)	12.7(2)
∠T2–P3	25.5(2)	18.6(1)
∠P1–P4	51.6(3)	-
∠P2–P5	61.8(2)	-

Absorption Spectra

In toluene, all compounds show a broad and structureless lowest-energy absorption band with large molecular extinction coefficients ranging from 32 000 to 42 000 M^{-1} cm^{-1} (Figure 2). Considering the push-pull structures of these compounds, their absorption bands are assigned as ICT transitions. The absorption maxima (λ_{abs}) of **1–3** are located at 433, 452 and 457 nm, respectively (Table 2). The very close values of λ_{abs} for **2** and **3** indicates that $(Pfp)_2B$ and $(Tfp)_2B$ have similar acceptor strengths. A spectral red shift of *ca.* 20 nm (1000 cm^{-1}) from **1** to **2** and **3** shows the effect of increased acceptor strength; however, the absorption maximum of **4** is significantly red shifted to 507 nm (a further 2200 cm^{-1}), indicating that $(FMes)_2B$ is a much stronger acceptor than Mes_2B, $(Pfp)_2B$, and $(Tfp)_2B$. By enhancing the donor strength, the λ_{abs} of **5** (484 nm) and **6** (487 nm) are red shifted by *ca.* 30 nm (1400 cm^{-1}) compared to those of the corresponding Tpa-substituted analogues, **2** and **3**, but still not to the same extent as **4**. The λ_{abs} of these compounds are slightly dependent on the solvent polarities: from toluene to CH_3CN, a negative shift of 5–23 nm was observed.

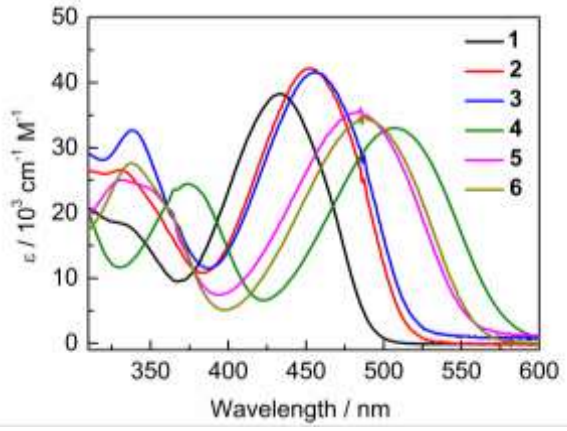

Figure 2. UV-visible absorption spectra of **1–6** in toluene.

Table 2. Photophysical data for **1–6** in solution and in the solid state at room temperature.

Compound	Medium	λ_{abs} / nm[a]	λ_{em} / nm	Stokes shift / cm^{-1}	Φ_F[b]	τ_F / ns	k_r / 10^7 s^{-1}	k_{nr} / 10^7 s^{-1}
1	toluene	433	504	3300	0.95	1.87	50.8	2.67
	THF	433	546	4800	0.96	2.46	39.0	1.63
	CH_3CN	428	599	6700	0.92	3.20	28.8	2.50
	solid	-	548	-	0.30	-	-	-
2	toluene	452	530	3300	0.98	2.19	44.7	0.91
	THF	449	583	5100	1.00	2.91	34.3	0.00
	CH_3CN	439	638	7100	0.96	3.59	26.7	1.11
	solid	-	545	-	0.46	-	-	-
3	toluene	457	535	3200	0.96	2.23	43.0	1.79
	THF	451	583	5000	0.93	2.89	32.1	2.42
	CH_3CN	442	636	6900	0.85	3.51	24.2	4.27
	solid	-	563	-	0.27	-	-	-
4	toluene	507	644	4200	_[c]	_[c]	-	-
	THF	495	_[c]	_[c]	_[c]	_[c]	-	-
	CH_3CN	484	_[c]	_[c]	_[c]	_[c]	-	-
	solid	-	646	-	0.31	-	-	-
5	toluene	484	582	3900	0.93	2.69	34.6	2.60
	THF	484	664	5600	0.87	3.53	24.6	3.68
	CH_3CN	478	745	7500	0.48	2.58	18.6	20.2
	solid	-	635	-	0.23	-	-	-
6	toluene	487	588	3500	0.95	2.76	34.4	1.81
	THF	485	666	5600	0.80	3.42	23.4	5.85
	CH_3CN	474	744	7700	0.27	1.56	17.3	46.8
	solid	-	618	-	0.05	-	-	-

[a] Lowest-energy absorption maximum. [b] Absolute fluorescence quantum yields measured using an integrating sphere. [c] Not determined due to very weak emission.

DFT and TD-DFT Calculations

To understand further the electronic structures of these compounds, and to examine the orbitals involved in the electronic transitions, we carried out DFT (B3LYP/6-31G(d)) and TD-DFT (CAM-B3LYP/6-31G(d)) calculations for **1**, **2**, **4** and **5**. Considering the quite similar profiles and peak wavelengths of the absorption spectra of **2** and **3**, and **5** and **6**, the electronic structures of **3** and **6** are expected to be similar to those of **2** and **5**, respectively. TD-DFT calculations show that the $S_1 \leftarrow S_0$ transitions of these compounds have large oscillator strengths, greater than or equal to 1.466, and the excitation wavelengths for the $S_1 \leftarrow S_0$ transitions are 392, 405, 424 and 410 nm for **1**, **2**, **4** and **5**, respectively (Table 3). These calculated values overestimate the experimental λ_{abs} values by 0.30–0.46 eV, which is not untypical for such systems.[9j,15] Importantly, the results reproduce the variation in observed values of λ_{abs}. According to the calculations, for all three compounds, the $S_1 \leftarrow S_0$ transitions are predominantly LUMO ← HOMO with a small contribution from LUMO ← HOMO–1. As can be seen from Figure 3, the HOMO and HOMO–1 are distributed on the donor and the bithienyl-spacer for all compounds, while the LUMO is mainly distributed on the acceptor and the bithienyl-spacer. Therefore, these transitions possess ICT character, which is consistent with our assignment of the experimental lowest-energy absorption bands as being due to ICT.

Table 3. TD-DFT calculated photophysical data for **1**, **2**, **4** and **5** at the CAM-B3LYP/6-31G(d) level.

	Transition (*f*)	*E* / eV[a]	λ / nm[a]	Dominant Components[b]
1	$S_1 \leftarrow S_0$	3.16 (2.86)	392 (433)	LUMO ← HOMO (70%)
	(1.618)			LUMO ← HOMO–1 (20%)
2	$S_1 \leftarrow S_0$	3.06 (2.74)	405 (452)	LUMO ← HOMO (66%)
	(1.676)			LUMO ← HOMO–1 (22%)
4	$S_1 \leftarrow S_0$	2.93 (2.50)	424 (507)	LUMO ← HOMO (63%)
	(1.470)			LUMO ← HOMO–1 (23%)
5	$S_1 \leftarrow S_0$	3.02 (2.56)	410 (484)	LUMO ← HOMO (77%)
	(1.466)			LUMO ← HOMO–1 (14%)

[a] Values in parentheses are experimental longest-wavelength absorption maxima in toluene. [b] Components with greater than 10% contribution shown. Percentage contribution approximated by 2 x $(c_i)^2$ x 100%, where c_i is the coefficient for the particular orbital rotation.

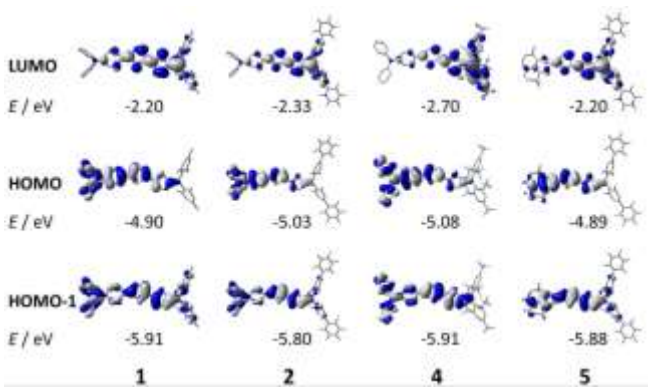

Figure 3. DFT (B3LYP/6-31G(d)) calculated frontier orbitals for **1**, **2**, **4** and **5**. Surface isovalue: ± 0.02 [$e\ a_0^{-3/2}$].

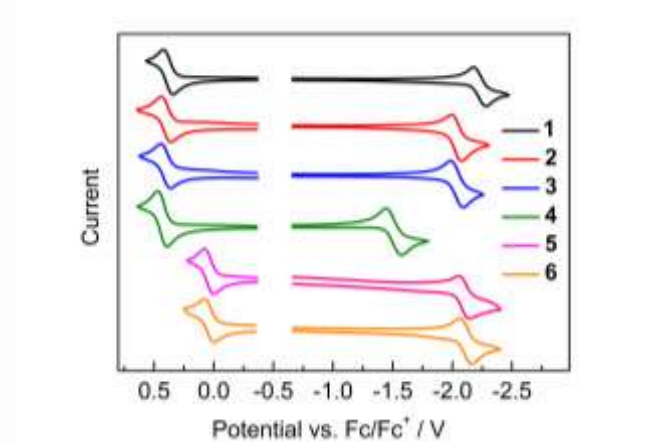

Figure 4. Cyclic voltammograms of **1**–**6**. Oxidation and reduction processes were measured in CH_2Cl_2 and THF, respectively.

Electrochemistry

Electrochemical measurements were carried out to evaluate further the acceptor strength and to confirm experimentally the influence of different donors and acceptors on the HOMO and LUMO levels and energy gaps. Cyclic voltammetry measurements (Figure 4 and Table 4) show that both the reduction and oxidation processes of these compounds are reversible, indicating their bipolar character. Compared to **1** ($E_{red}^{1/2}$ = –2.23 V), compounds **2** ($E_{red}^{1/2}$ = –2.04 V) and **3** ($E_{red}^{1/2}$ = –2.04 V) are more easily reduced with reduction potentials positively shifted by *ca.* 0.2 V. The reduction of **4** ($E_{red}^{1/2}$ = –1.61 V) is much easier than that of **2** or **3**, exhibiting an $E_{red}^{1/2}$ positively shifted by *ca.* 0.4 V. These results confirm an increased acceptor strength in the order of $(Mes)_2B$ < $(Pfp)_2B$ ≈ $(Tfp)_2B$ << $(FMes)_2B$. The oxidation potentials of **1**–**4** are very similar, exhibiting little increase with enhanced acceptor strength and, thus, the donor and acceptor groups are relatively electronically decoupled in the ground state. The stronger Tmjul donor groups of **5** and **6** make their oxidation ($E_{ox}^{1/2}$ = +0.04 V) much easier than that of either **2** or **3** ($E_{ox}^{1/2}$ = +0.41 V) bearing triarylamine donors. The increased donor strength also has a slight influence on $E_{red}^{1/2}$, making the reduction of **5** and **6** slightly more difficult than that of either **2** or **3** by *ca.* 0.06 eV. From the electrochemical data, the HOMO and LUMO energy levels and energy gaps were calculated (Table 4). Compared to **1**, the LUMOs of **2** and **3** are stabilized by 0.19 eV, while their HOMO levels are stabilized by only 0.02 eV, resulting in reduced HOMO-LUMO gaps. Moving from **2** and **3** to **5** and **6**, the HOMOs are strongly elevated while LUMO levels are only slightly raised, further leading to reduced energy gaps. The extremely strong acceptor in **4** results in a significantly stabilized LUMO level, which serves as a key factor leading to its small energy gap, the smallest amongst the compounds presented here. Therefore, the energy gaps obtained from electrochemical measurements show the same trend as the optical band gaps.

Table 4. Cyclic voltammetric data,[a] and experimental HOMO and LUMO energies.

	$E_{ox}^{1/2}$ / V[b]	$E_{red}^{1/2}$ / V[c]	HOMO / eV[d]	LUMO / eV[d]	E_g / eV[e]
1	+0.39	–2.23	–5.19	–2.57	2.62 (2.53)
2	+0.41	–2.04	–5.21	–2.76	2.45 (2.42)
3	+0.41	–2.04	–5.21	–2.76	2.45 (2.39)
4	+0.43	–1.61	–5.23	–3.19	2.04 (2.14)
5	+0.04	–2.10	–4.84	–2.70	2.14 (2.24)
6	+0.04	–2.11	–4.84	–2.69	2.15 (2.21)

[a] Potentials are given *vs.* ferrocene/ferrocenium (Fc/Fc^+). [b] Measured in CH_2Cl_2. [c] Measured in THF. [d] Estimated assuming that the HOMO of Fc lies 4.8 eV below the vacuum level.[21] [e] Values in parentheses are optical band gaps calculated from the low-energy edge of the absorption spectra in toluene.

Photoluminescence

In solution, the emission wavelengths and observed emission colors of these compounds strongly depend on the solvent (Figure 5 and Table 2). With increased solvent polarity, the emission spectra of all of the compounds broaden and exhibit a significant red shift. This is attributed to a highly polarized ICT excited state, which is typical for D-π-A compounds. From toluene to CH_3CN, the emission maxima (λ_{em}) of **1** shifts from 504 to 599 nm (3100 cm^{-1}), and the color of the emission varies from green to orange. With its increased acceptor strength, **2** shows red-shifted emission in each solvent compared to **1**, exhibiting emission ranging from yellow-green to red with λ_{em} shifting from 530 to 638 nm. It is notable that compounds **1** and **2** show very high Φ_F values (0.92–1.00), even for the orange/red emission in polar solvents, which is remarkable and uncommon for push-pull systems, since emission from ICT states is usually quenched in more polar solvents. Only a few D-π-A type organoboron compounds showing solvent-independent Φ_F values close to unity have been reported.[8b] The emission spectra of **3** are similar to those of **2** in each solvent, consistent with their similar absorption

spectra, as discussed above. Compound **3** also has high Φ_F (0.85–0.96) values in all three solvents used; however, the emission is somewhat more easily quenched by polar CH_3CN compared to **1** and **2**. Compound **4**, with the strongest acceptor, displays a huge spectral red shift in toluene (λ_{em} = 644 nm) of 109–140 nm (3200–4300 cm^{-1}) compared to **1–3**. However, the emission of **4** in toluene is too weak to obtain a reliable value of Φ_F, and in more polar solvents, **4** is almost nonemissive. **5** and **6** have close λ_{em}, similar to the case of **2** and **3**, but their emission spectra are red-shifted and more sensitive toward solvents in relation to those of **2** and **3**, resulting from their stronger donors. These compounds show efficient orange (λ_{em} = *ca.* 585 nm) and red (λ_{em} = *ca.* 664 nm) emission in toluene and THF, respectively, with Φ_F ranging from 0.80–0.95. It is notable that these compounds display NIR (λ_{em} > 700 nm) emission in CH_3CN solution; this emission is somewhat quenched relative to that in less polar solvents (Table 2), but the Φ_F values are still good to high: 0.48 for **5** and 0.27 for **6**. As far as we are aware, these two compounds represent the first examples of three-coordinate boron compounds showing efficient NIR emission. We note, however, that a $(Mes)_2B$-containing iridium complex with two emission bands, one in the visible and one in the NIR region, was reported previously,[22] but this compound had a very low emission quantum yield of 5.7×10^{-4}. Moreover, recently, a borondipyrromethane derivative with $(Mes)_2B$-containing substituents was reported to show NIR emission; however, Φ_F was not mentioned.[23] In addition, in our previous work, we observed that Tpa-B$(FMes)_2$ displays NIR emission in THF; however, the Φ_F could not be determined because the emission was weak.[15] As compounds exhibiting NIR emission normally have relatively small Φ_F values, the quantum yield of **5** is among the highest reported,[24] to the best of our knowledge. In addition, our new NIR-emitting compounds also possess sizeable Stokes shifts of over 7000 cm^{-1} (*ca.* 270 nm) in CH_3CN. To understand the factors influencing the Φ_F values of the present systems, the Φ_F and fluorescence lifetimes (τ_F) of **1–3**, **5** and **6** were measured in all three solvents and the radiative (k_r) and nonradiative (k_{nr}) rate constants were calculated from these data. Due to its very weak emission, related data could not be obtained for **4**. The k_r values of these compounds show the following trends: 1) independent of solvent, k_r becomes smaller in the order of **1** > **2** ≈ **3** > **5** ≈ **6**, due to enhanced push-pull character; and 2) for each compound, k_r decreases with increased solvent polarity. The k_{nr} values of **1–3** are very small and do not show obvious changes between the three solvents, which results in high and solvent-independent Φ_F values for these compounds. In contrast, both **5** and **6** possess obviously increased k_{nr} values upon changing from toluene to CH_3CN solutions, with a more significant increase for **6**. The combined decrease in k_r and increase in k_{nr} with increasing solvent polarity leads to the relatively low Φ_F values of **5** and **6** in polar solvents, while the lower value of Φ_F for **6** in CH_3CN compared to **5** is attributed to the larger increase of k_{nr}. As for compound **4**, with the strongest push-pull character, as deduced from its significantly red-shifted absorption and emission spectra, the very weak emission is possibly related to a fairly small k_r value, caused by a twisted ICT (TICT) excited state, which could restrict the radiative deactivation of the S_1 state. Our previous study of Tpa–B$(FMes)_2$ showed that this compound has a highly twisted geometry in the S_1 excited state with a large deformation of the B$(FMes)_2$ group, which forms even in the gas phase.[15] To investigate whether the same process occurs for compound **4** of the present study, the excited-state (S_1) structure of this compound has been calculated using TD-DFT optimization (CAM-B3LYP/6-31G(d)). In the relaxation process from the S_1 Franck-Condon state following absorption, one FMes group rotates towards a more planar conformation (50.7 to 24.8°), while the second FMes group rotates somewhat and the bithienyl unit rotates to a significantly larger dihedral angle with respect to the BC_3 plane (63.8 to 74.9° and 19.3 to 76.7°, respectively. Figure S5); therefore, the S_1 state of **4** is described as a TICT state and is analogous to that observed for Tpa–B$(FMes)_2$. In the TICT state, there is electronic decoupling between the molecular orbitals involved in the emission ($S_1 \rightarrow S_0$) process (Figure S6), leading to a small oscillator strength of 0.035, consistent with the observed weak emission from this state in solution. This is in contrast to the allowed $S_1 \leftarrow S_0$ transition at the more planar ground-state geometry, which has a large oscillator strength of 1.470.

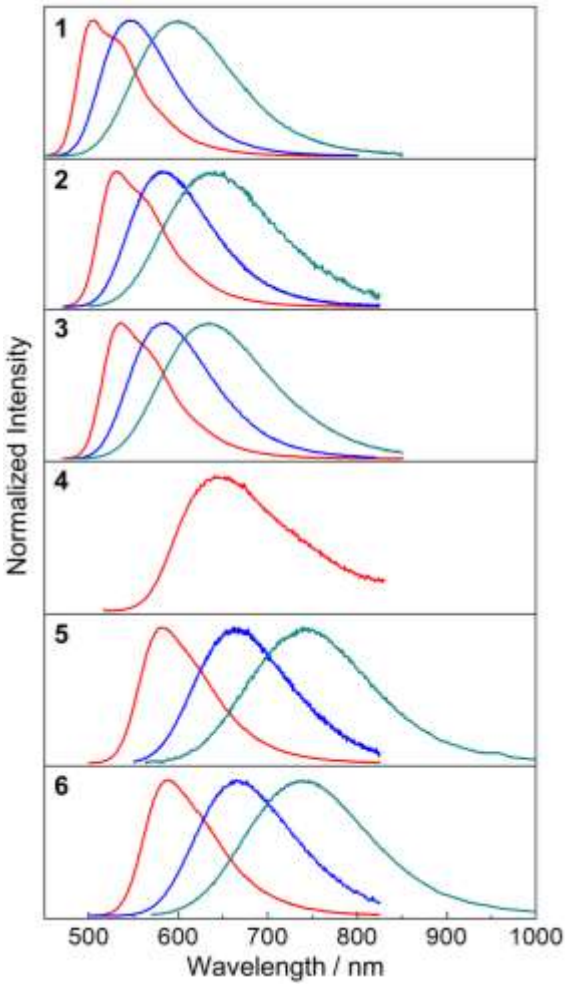

Figure 5. Emission spectra of **1–6** in toluene (red), THF (blue) and CH_3CN (green).

Because binding of anions to the Lewis acidic boron atom in the acceptor group occupies the previously vacant p_z-orbital thus destroying its accepting ability, this can be used to confirm the

ICT nature of the optical transitions. The different push-pull strengths of these compounds lead to different changes in emission color upon treatment with fluoride in THF. As can be seen from Figure 6, after an excess of fluoride was added to the solution, the emission of **1**, **2** and **5** changed from yellow-green to blue, yellow-orange to blue, and red to blue, respectively. A ^{19}F NMR study of **2** in CD_2Cl_2 confirmed that a 1:1 complex between the compound and fluoride was formed and that complete recovery of **2** can be achieved by washing with water (Figure S7). These results clearly confirmed that the original emission of these compounds come from an ICT state. The gradually larger color difference upon fluoride binding from **1** to **2** to **5** can be easily understood: initially, the enhanced push-pull character from **1** to **2** to **5** leads to red-shifted ICT emission; after fluoride is bound to the boron atom of the acceptor, the original ICT state cannot be formed; therefore, bright blue emission arising from the electronic transition within the donor-spacer moiety is observed. The emission-color change from red to blue for **5** is particularly remarkable. Such a large color difference has not been observed in sensing studies of three-coordinate-boron systems to the best of our knowledge. The distinct color change and the bright emission of both free and bound states facilitates naked-eyed recognition.[4c] Considering the similar photophysical properties of **2** and **3** and of **5** and **6** in THF, compounds **3** and **6** are expected to have responses similar to **2** and **5**, respectively. Compound **4** is non-emissive in THF; however, bright blue emission is observed after fluoride binding (Figure 7). Such a "turn-on" response behavior[5c,25] is quite different from the case of the other compounds. The elimination of the non-emissive ICT state of **4** upon fluoride binding and the generation of an emissive state similar to those observed for fluoride-bound **1**, **2** and **5** reasonably explains the "turn-on" response behavior. Following fluoride binding, **4** could not be recovered by washing with water; instead, excess BF_3•OEt_2 was used to extract the more strongly bound fluoride, which further demonstrates the enhanced Lewis acidity of **4** compared to **2** (Figure S8). We suggest that the binding of fluoride used herein to confirm our interpretation of the photophysical studies could possibly be applied to the development of efficient fluoride probes, but we note that this is already a very mature area.[3b-d,f,4a-c,5a-e,6,11,14g]

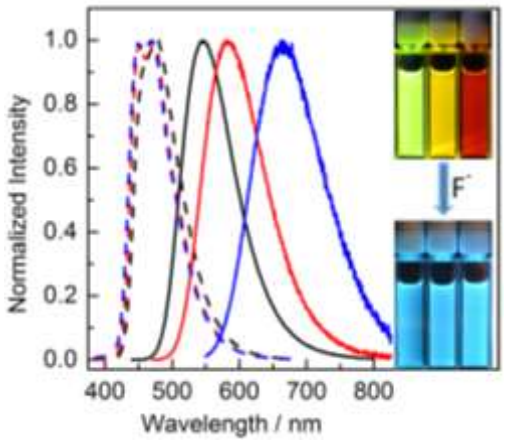

Figure 6. Emission spectra of **1** (black), **2** (red) and **5** (blue) before (solid line) and after (dashed line) excess F^- (> 5 eq.) is added to the THF solution. The inset shows the emission-color changes of **1** (left), **2** (middle) and **5** (right) following F^- binding in THF under 365 nm UV-light irradiation.

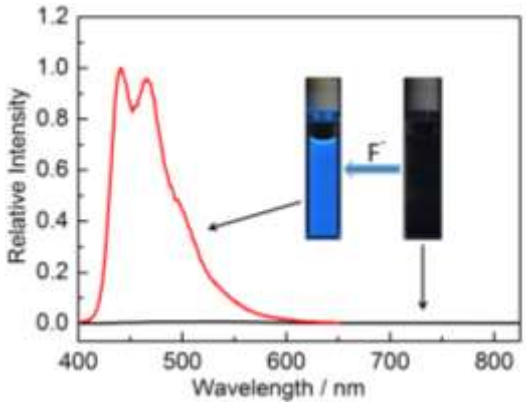

Figure 7. Emission spectra of **4** before (black line) and after (red line) excess F^- (> 5 eq.) is added to the THF solution. The inset shows the "turn-on" of fluorescence after F^- binding under 365 nm UV irradiation.

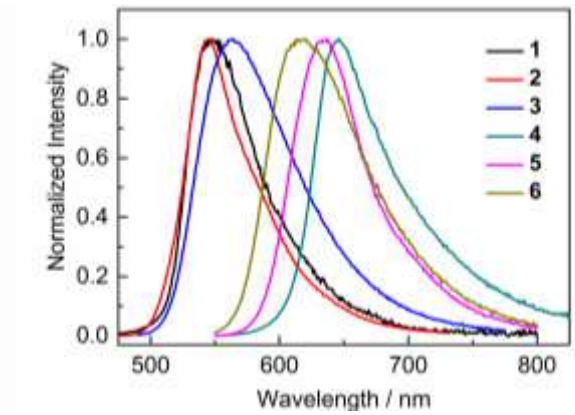

Figure 8. Emission spectra of solid (powder) samples of **1**–**6**.

As solid powders, **1**–**3** show yellow emission, while **4**–**6** show red emission. The emission maxima are located at 548, 545, 563, 646, 635 and 618 nm for **1**–**6**, respectively (Figure 8). The solid-state Φ_F values of **1**–**3**, **5** and **6** are 0.30, 0.46, 0.27, 0.23 and 0.05, respectively, which, although still moderate, are much lower than those of their solutions (Table 2). Such aggregation-induced quenching of fluorophores is commonly observed in the solid state.[26] Interestingly, compound **4** shows the opposite behavior, exhibiting a much higher Φ_F value (0.31) in the solid state than in solution: such behavior is known as aggregation-induced emission (AIE),[26a,27] but has rarely been observed for three-coordinate boron compounds.[28] Several studies indicate that the AIE phenomenon of compounds possessing donor and acceptor subunits may be caused by restricted formation of a TICT state,[29] which is likely the reason for the AIE of **4**. As discussed in regard to the solution photophysics, the nonemissive nature of **4** in solution should be related to a highly twisted ICT excited state geometry with a low $S_1 \rightarrow S_0$ oscillator strength. However, as disclosed in the crystal structure of **4**, the NC_3-Ph-dithienyl-BC_3 moiety is relatively planar with small interplanar dihedral angles in the ground state, close to the optimized S_0 structure. Once the compound is excited in the solid state, the rigid environment restricts the formation of the TICT state; therefore, more efficient

emission might be expected from this geometry. The low-temperature (77 K) emission spectrum of **4** in frozen toluene (λ_{em} = 597 nm) shows a significant blue shift of 47 nm (1200 cm^{-1}) compared to the solution spectrum in toluene (Figure 9), which is similar to the behavior of Tpa–B(FMes)$_2$ and consistent with the lack of formation of a TICT state in a rigid environment.[15] In addition, the emission in frozen toluene solution shows significantly increased intensity, similar to the case in the rigid solid and consistent with our hypothesis of an efficient emission from a more planar excited-state conformation. We note that λ_{em} of **4** in the solid-state is red-shifted compared to that in frozen toluene by 49 nm (1300 cm^{-1}), which may be related to aggregation in the solid state. Compounds **4** (Φ_F = 0.23) and **5** (Φ_F = 0.31), with their efficient red emission in the solid state, are especially interesting, given the lack of efficient red emitters based on organoboron compounds.

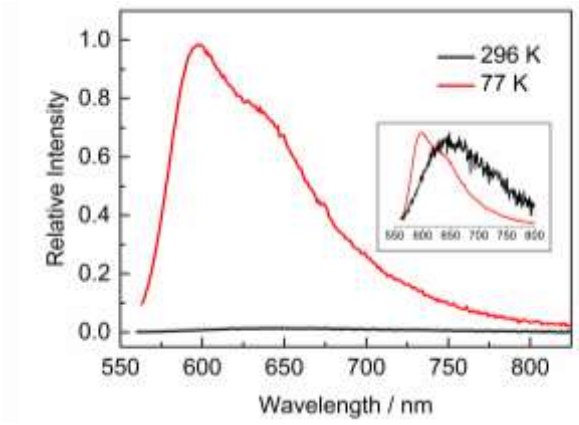

Figure 9. Emission spectra of **4** in toluene at different temperatures. Inset: Normalized spectra showing the blue-shift upon cooling.

Conclusion

A series of donor-bithienyl-acceptor compounds containing Ar_2B acceptor and arylamine donor groups was synthesized. The acceptor strength was systematically tuned by varying Ar_2B, namely by using Ar = mesityl ((Mes)$_2$B), 2,6-dimethyl-4-pentafluoropenylbenzene ((Pfp)$_2$B), 2,6-dimethyl-4-(3,5-bis(trifluoromethyl)phenyl)benzene ((Tfp)$_2$B) and 2,4,6-tris(trifluoromethyl)benzene ((FMes)$_2$B). Tuning the donor strength by exchange of a triphenylamine donor for a stronger 1,1,7,7-tetramethyljulolidine donor gave further fine control over the optoelectronic properties. The key to the high-yield syntheses of these compounds was the use of iridium-catalyzed C–H borylation, which was successfully employed in the process of derivatizing both the boryl acceptors and the tetramethyljulolidine donor.

The acceptor groups were evaluated using a complementary combination of crystallographic, photophysical, electrochemical and theoretical studies, which established that the order of increasing strength is (Mes)$_2$B < (Pfp)$_2$B ≈ (Tfp)$_2$B << (FMes)$_2$B. In CH_3CN, near-infrared emission with quantum yields of 0.27–0.48 was obtained for derivatives containing the moderately strong (Pfp)$_2$B and (Tfp)$_2$B acceptors and tetramethyljulolidine donors, which is the first time such efficient low-energy emission has been observed from a three-coordinate organoboron system. A compound containing the strongest acceptor, (FMes)$_2$B, and a triphenylamine donor suffers from strongly quenched emission in solution, while the analogous derivatives containing (Pfp)$_2$B and (Tfp)$_2$B, have near-unity quantum yields, even in polar CH_3CN solution, making them particularly attractive for practical applications. Although very high quantum yields (>0.80) were obtained for (Pfp)$_2$B- and (Tfp)$_2$B-containing compounds with tetramethyljulolidine donors in toluene and THF, reduced values of k_r and increased values of k_{nr} led to quantum yields in CH_3CN solution being decreased by a factor of approximately two to three. Thus, our systematic studies suggest that employing donors and acceptors of medium strength is essential for achieving efficient emission in polar solvents, insight that should facilitate the future design of bright, organoboron-based NIR emitters. Efficient solid-state red emission was observed for some derivatives and interesting aggregation-induced emission of **4** containing the (FMes)$_2$B group was studied. Moreover, each compound showed a strong and clearly visible response to the addition of fluoride, with either a large emission-color change, *e.g.* from red to blue or turn-on fluorescence.

Experimental Section

General Information

(FMes)$_2$BF (bis(fluoromesityl)boron fluoride),[30] (2,2'-bithiophen)-5-ylboronic acid,[31] 5-iodo-2,2'-bithiophene[32] and {Ir(μ-OMe)(COD)}$_2$[33] were prepared according to literature procedures. All other starting materials were purchased from commercial sources and were used without further purification. The organic solvents for synthetic reactions and for photophysical and electrochemical measurements were HPLC grade, further treated to remove trace water using an Innovative Technology Inc. Pure-Solv Solvent Purification System and deoxygenated using the freeze-pump-thaw method. All synthetic reactions were performed in an Innovative Technology Inc. glovebox or under an argon atmosphere using standard Schlenk techniques. ^{1}H, ^{13}C{^{1}H} and ^{11}B NMR spectra were measured on either a Bruker Avance 500 (^{1}H, 500 MHz; ^{13}C, 125 MHz; ^{11}B, 160 MHz) or Bruker Avance 300 (^{1}H, 300 MHz; ^{13}C, 75 MHz; ^{11}B, 96 MHz) NMR spectrometer. ^{19}F{^{1}H} and ^{19}F NMR spectra were measured on either a Bruker Avance 200 (^{19}F, 188 MHz) or Bruker Avance 500 (^{19}F, 470 MHz) NMR spectrometer. The abbreviation dm stands for doublet of multiplets. Mass spectra were recorded on Agilent 7890A/5975C Inert GC/MSD or Varian 320MS-GC/MS systems operating in EI mode. Elemental analyses were performed on a Leco CHNS-932 Elemental Analyzer.

Single-Crystal X-ray Diffraction

Crystals suitable for single-crystal X-ray diffraction were selected, coated in perfluoropolyether oil, and mounted on MiTeGen sample holders. Diffraction data of Tmjul-Bpin and **2** were collected on a Bruker D8 Quest three-circle diffractometer utilizing mirror-monochromated Mo Kα radiation (λ = 0.71073 Å) from an IμS microfocus sealed X-ray tube (Incoatec, Germany) operated at 50 kV and 1 mA, and equipped with a Photon area detector. Diffraction data of **4** were collected on a Nonius Kappa three circle diffractometer utilizing graphite monochromated Mo Kα radiation (λ = 0.71073 Å) from a rotating anode tube run at 50 kV and 30 mA, equipped with an APEXII area detector. Both instruments were operated with an open-flow N_2 Cryoflex II (Bruker) device and measurements were performed at 100 K. For data reduction, the Bruker Apex2 software suite (Bruker AXS) was used. Subsequently, utilizing Olex2,[34] the structures were solved using the Olex2.solve charge-flipping algorithm, and were subsequently refined with Olex2.refine using Gauss-Newton minimization. All non-hydrogen atom positions were located from the Fourier maps and refined anisotropically. Hydrogen atom positions were calculated using a riding model in geometric positions and refined isotropically.

CCDC-1025373 (Tmjul–Bpin), 1025372 (**2**) and 1025371 (**4**) contain the supplementary crystallographic data for this paper. These data can be obtained free of charge from The Cambridge Crystallographic Data Centre via www.ccdc.cam.ac.uk/data_request/cif.

General Photophysical Measurements

All solution-state measurements were made in standard quartz cuvettes (1 cm x 1 cm cross-section). UV–visible absorption spectra were recorded using an Agilent 8453 diode array UV-visible spectrophotometer. The emission spectra were recorded using an Edinburgh Instruments FLSP920 spectrometer equipped with a double monochromator for both excitation and emission, operating in right-angle geometry mode, and all spectra were fully corrected for the spectral response of the instrument. All solutions used in photophysical measurements had a concentration lower than 10^{-5} M.

Fluorescence Quantum Yield Measurements

The fluorescence quantum yields of solutions and powders were measured using a calibrated integrating sphere (150 mm inner diameter) from Edinburgh Instruments combined with the FLSP920 spectrometer described above. For solution-state measurements, the longest-wavelength absorption maximum of the compound in the respective solvent was chosen as the excitation wavelength, while for solid-state (powder) measurements, the longest-wavelength absorption maximum in toluene was selected.

Fluorescence Lifetime Measurements

Fluorescence lifetimes were recorded using the time-correlated single-photon counting (TCSPC) method using an Edinburgh Instruments FLS980 spectrometer equipped with a high speed photomultiplier tube positioned after a single emission monochromator. Measurements were made in right-angle geometry mode, and the emission was collected through a polarizer set to the magic angle. Solutions were excited with a 418 nm pulsed diode laser at repetition rates of 10 or 20 MHz, as appropriate. The full-width-at-half-maximum (FWHM) of the pulses from both diode lasers was *ca.* 75 ps with an instrument response function (IRF) of *ca.* 230 ps FWHM. The IRFs were measured from the scatter of a LUDOX aqueous suspension at the excitation wavelength. Decays were recorded to at least 4 000 counts in the peak channel with a record length of at least 1 000 channels. The band pass of the monochromator was adjusted to give a signal count rate of <60 kHz. Iterative reconvolution of the IRF with one or two decay functions and non-linear least-squares analysis were used to analyze the data. The quality of all decay fits was judged to be satisfactory, based on the calculated values of the reduced χ^2 and Durbin-Watson parameters and visual inspection of the weighted residuals.

Electrochemical Measurements

All cyclic voltammetry experiments were conducted in an argon-filled glovebox using a Gamry Instruments Reference 600 potentiostat. A standard three-electrode cell configuration was employed using a platinum disk working electrode, a platinum wire counter electrode, and a silver wire reference electrode separated by a Vycor frit. Compensation for resistive losses (*IR* drop) was employed for all measurements. A 0.1 M solution of $[NBu_4][PF_6]$ was used as the supporting electrolyte. A scan rate of 250 mV s^{-1} was adopted.

Theoretical Studies

All calculations (DFT and TD-DFT) were carried out with the program package Gaussian 09 (Rev. B.01)[35] and were performed on a parallel cluster system. Gaussview 5.0 was used to visualize the results, to measure calculated distances and bond lengths, and to plot orbital surfaces. The ground-state geometries were optimized without symmetry constraints using the B3LYP functional[36-38] in combination with the 6-31G(d) basis set.[39] The molecular structures of **2** and **4** as determined by X-ray crystallography were used as the input for optimizing their ground-state geometries; the input structure of **1** was obtained by replacing the C_6F_5 groups of **2** with methyl groups; and the input structure of **5** was obtained by exchanging the Tpa group of **2** for a Tmjul group. The optimized geometries were confirmed to be local minima by performing frequency calculations and obtaining only positive (real) frequencies. Based on these optimized structures, the lowest-energy gas-phase vertical transitions were calculated (singlets, six states) by TD-DFT using the Coulomb-attenuated functional CAM-B3LYP[40] in combination with the 6-31G(d) basis set as this pairing has been shown to be effective for ICT systems.[41] The S_1 state of **4** was optimized using TD-DFT optimization at the CAM-B3LYP/6-31G(d) level of theory with six singlet states. No symmetry constraint was used in any of the calculations.

Synthesis

5-(4-Bisphenylaminophenyl)-2,2'-bithiophene (Tpa–Th–Th).[42] 4-Bromo-*N*,*N*-diphenylaniline (926 mg, 2.86 mmol), [(2,2'-bithiophene)-5-yl]boronic acid (500 mg, 2.38 mmol), Na_2CO_3 (1.26 g, 11.9 mmol), $[Pd(PPh_3)_4]$ (110 mg, 0.10 mmol), THF (35 mL), and degassed H_2O (6 mL) were added to a flask. The mixture was heated at reflux for 24 h and then cooled to r.t. Water and diethyl ether were added to the mixture for extraction. The organic phase was evaporated to dryness, and the residue was purified by column chromatography (silica gel, 8:1 hexane/CH_2Cl_2). Subsequent crystallization from hexane provided the title compound as a yellow solid (695 mg, 71%). ^{1}H NMR (500 MHz, DMSO-d_6, ppm): δ 7.58 (d, J = 8 Hz, 2 H), 7.52 (d, J = 4 Hz, 1 H), 7.38–7.29 (m, 7 H), 7.11–7.06 (m, 7 H), 6.99 (d, J = 8 Hz, 2 H). ^{13}C{^{1}H} NMR (125 MHz, THF-d_8, ppm): 148.5, 148.4, 143.8, 138.3, 136.7, 130.1, 129.1, 128.6, 127.1, 125.3 (2 C, overlap), 125.1, 124.5, 124.2, 124.0, 123.8. MS (EI$^+$) *m*/*z*: 409 [M]$^+$. Anal. Calcd (%) for $C_{26}H_{19}NS_2$: C, 76.25; H, 4.68; N, 3.42; S, 15.66. Found: C, 76.91; H, 4.81; N, 3.46; S, 15.90.

1,1,7,7-Tetramethyljulolidin-9-yl boronic acid pinacol ester (Tmjul–Bpin). 1,1,7,7-Tetramethyljulolidine (6.00 g, 26.2 mmol), bis(pinacolato)diboron (B_2pin_2, 8.65 g, 34.1 mmol), $[Ir(\mu\text{-OMe})(COD)]_2$ (174 mg, 0.26 mmol), 4,4'-di-*tert*-butyl-2,2'-bipyridine (dtbpy) (138 mg, 0.51 mmol) and hexane (36 mL) were added to a flask. The reaction mixture was heated at 80 °C for 48 h, then cooled to r.t. and then further cooled in ice-water to crystallize the product. The mixture was filtered, and the solid product was washed with cold hexane (80 mL) and dried in vacuum to provide the title compound as an off-white solid (8.22 g, 88%). ^{1}H NMR (300 MHz, C_6D_6, ppm): δ 8.05 (s, 2 H), 2.86 (t, J = 6 Hz, 4 H), 1.50 (t, J = 6 Hz, 4 H), 1.20 (s, 12 H), 1.19 (s, 12 H). ^{13}C{^{1}H} NMR (125 MHz, CD_2Cl_2, ppm): δ 143.5, 130.8, 129.5, 114.3 (br), 83.3, 47.1, 37.1, 32.4, 31.2, 25.1.^{11}B NMR (96 MHz, C_6D_6, ppm): δ 31.3 (s, 1 B). MS (EI$^+$) *m*/*z*: 355 [M]$^+$. Elem. Anal. Calcd (%) for $C_{22}H_{34}BNO_2$: C, 74.37; H, 9.64; N, 3.94. Found: C, 74.23; H, 9.58; N, 3.96.

5-(1,1,7,7-Tetramethyljulolidin-9-yl)-2,2'-bithiophene (Tmjul–Th–Th). Tmjul–Bpin (3.00 g, 8.45 mmol), 5-iodo-2,2'-bithiophene (2.95g, 10.1mmol), Ag_2CO_3 (5.80 g, 21.0 mmol), $[Pd(PPh_3)_4]$ (484 mg, 0.42 mmol) and THF (45 mL) were added to a flask. The mixture was heated at reflux for 24 h, cooled to r.t. and filtered. The filtrate was evaporated to dryness, and the residue was purified by column chromatography (Al_2O_3, 8:1 hexane/CH_2Cl_2) and subsequent crystallization from hexane to provide the title compound as a yellow solid (1.80 g, 54%). ^{1}H NMR (500 MHz, THF-d_8, ppm): δ 7.26 (s, 2 H), 7.24 (dd, J = 5, 1 Hz, 1 H), 7.15(dd, J = 4, 1 Hz, 1 H), 7.09 (d, J = 4 Hz, 1 H), 7.03 (d, J = 4 Hz, 1 H), 6.98 (dd, J = 5, 4 Hz, 1 H), 3.20–3.18 (m, 4 H), 1.77–1.74 (m, 4 H), 1.30 (s, 12 H). ^{13}C{^{1}H} NMR (126 MHz, THF-d_8, ppm): δ 146.2, 141.1, 138.7, 134.3, 131.1, 128.3, 124.9, 124.1, 123.2, 122.2, 122.1, 121.2, 47.2, 37.6, 32.8, 31.3. MS (EI$^+$) *m*/*z*: 393 [M]$^+$. Anal. Calcd (%) for $C_{24}H_{27}NS_2$: C, 73.23; H, 6.91; N, 3.56; S, 16.29. Found: C, 73.05; H, 6.85; N, 3.56; S, 16.05.

4-Bromo-3,5-dimethylphenyl boronic acid pinacol ester (4-Br-3,5-Me$_2$-Ph-Bpin). 2,6-Dimethylbromobenzene (18.5 g, 100 mmol), B_2pin_2 (33.0 g, 130 mmol), $[Ir(\mu\text{-OMe})(COD)]_2$ (333 mg, 0.50 mmol), dtbpy (403 mg, 1.50 mmol) and hexane (116 mL) were added to a flask. The reaction mixture was heated at 80 °C for 65 h, cooled to r.t., and then filtered through a short silica-gel pad. The obtained solution was evaporated to give an oil, which was purified by column chromatography (silica gel, hexane). The obtained oily product solidified under vacuum to give the title compound as a white solid (29.3 g, 95%). ^{1}H NMR (500 MHz, CD_2Cl_2, ppm): δ 7.49 (s, 2 H), 2.43 (s, 6 H), 1.34 (s, 12 H). ^{13}C{^{1}H} NMR (126 MHz, CD_2Cl_2, ppm): δ 138.1, 134.7, 131.6, 127.9 (br), 84.3, 25.1, 23.9. ^{11}B NMR (160 MHz, CD_2Cl_2, ppm): δ 29.9 (s, 1 B). MS (EI$^+$) *m*/*z*: 310 [M]$^+$. Anal. Calcd (%) for $C_{14}H_{20}BBrO_2$: C, 54.06; H, 6.48. Found: C, 54.45; H, 6.55.

4-Perfluorophenyl-2,6-dimethylbromobenzene (Pfp–Br). 4-Br-3,5-Me$_2$-Ph-Bpin (8.00 g, 25.8 mmol), C_6F_5I (12.9 g, 43.9 mmol), Ag_2CO_3 (17.8 g, 64.5 mmol), $[Pd(PPh_3)_4]$ (1.48 g, 1.28 mmol) and THF (120 mL) were added to a flask. The mixture was heated at reflux for 25 h, cooled to r.t., and then filtered. The filtrate was evaporated to dryness, and the residue was purified by column chromatography (silica gel, hexane) to provide the title compound as a white

solid (7.25 g, 80%). ^{1}H NMR (500 MHz, $CDCl_3$, ppm): δ 7.15 (s, 2 H), 2.49 (s, 6 H). $^{13}C\{^1H\}$ NMR (126 MHz, $CDCl_3$, ppm): δ 144.2 (dm, $^1J_{CF}$ = 248 Hz), 140.6 (dm, $^1J_{CF}$ = 254 Hz), 139.2, 138.0 (dm, $^1J_{CF}$ = 251 Hz), 129.7, 129.1, 124.9, 115.4 (td, $^2J_{CF}$ = 17 Hz, $^3J_{CF}$ = 4 Hz), 24.0. $^{19}F\{^1H\}$ NMR (188 MHz, $CDCl_3$, ppm): δ –142.9 (dd, J = 23, 8 Hz, 2 F), –155.3 (t, J = 21 Hz, 1 F), –162.0 to –162.2 (m, 2 F). MS (EI^+) m/z: 350 $[M]^+$. Anal. Calcd (%) for $C_{14}H_8BrF_5$: C, 47.89; H, 2.30. Found: C, 47.98; H, 2.46.

4-(3,5-Bis(trifluoromethyl)phenyl)-2,6-dimethylbromobenzene (Tfp–Br). 4-Br-3,5-Me_2-Ph-Bpin (3.10 g, 10.0 mmol), 3,5-bis(trifluoromethyl)iodobenzene (5.78 g, 17.0 mmol), Ag_2CO_3 (6.90 g, 25.0 mmol), $[Pd(PPh_3)_4]$ (577 mg, 0.50 mmol) and THF (45 mL) were added to a flask. The mixture was heated at reflux for 21 h, cooled to r.t. and then filtered. The filtrate was evaporated to dryness, and the residue was purified by column chromatography (silica gel, hexane) and subsequent crystallization from methanol to provide the title compound as a white solid (3.11 g, 79%). ^{1}H NMR (500 MHz, CD_2Cl_2, ppm): δ 8.05 (m, 2 H), 7.91 (m, 1 H), 7.35 (m, 2 H), 2.51(m, 6 H). $^{13}C\{^1H\}$ NMR (126 MHz, CD_2Cl_2, ppm): δ 142.9, 139.9, 137.0, 132.5 (q, $^2J_{CF}$ = 33 Hz), 128.9, 127.5 (m), 127.2, 124.0 (q, $^1J_{CF}$ = 273 Hz), 121.5 (septet, $^3J_{CF}$ = 4 Hz), 24.2. $^{19}F\{^1H\}$ NMR (188 MHz, C_6D_6, ppm): δ –61.4 (s, 6 F). MS (EI^+) m/z: 396 $[M]^+$. Anal. Calcd (%) for $C_{16}H_{11}BrF_6$: C, 48.39; H, 2.79. Found: C, 48.83; H, 2.79.

Tpa–Th–Th–B(Mes)$_2$ (1). n-BuLi (2.5 M in hexane, 0.23 mL, 0.58 mmol) was added to a THF (5 mL) solution of Tpa–Th–Th (216 mg, 0.53 mmol) at –78 °C, and then the mixture was stirred at this temperature for 1 h. After a THF (2 mL) solution of $(Mes)_2BF$ (170 mg, 0.63 mmol) was added, the mixture was slowly warmed to r.t. and stirred for 2 h. The solvent was removed under vacuum, and the residue was purified by column chromatography (silica gel, 4:1 hexane/CH_2Cl_2) and subsequent precipitation from diethyl ether by addition of methanol to provide **1** as a yellow solid (303 mg, 87%).^{1}H NMR (500 MHz, THF-d_8, ppm): δ 7.51 (d, J = 9 Hz, 2 H), 7.39 (d, J = 4 Hz, 1 H), 7.33–7.32 (m, 2 H), 7.27–7.23 (m, 5 H), 7.09–7.07 (m, 4 H), 7.03–7.00 (m, 4 H), 6.81 (s, 4 H), 2.27 (s, 6 H), 2.13 (s, 12 H). $^{13}C\{^1H\}$ NMR (126 MHz, CD_2Cl_2, ppm): δ 150.4, 149.1 (br), 148.2, 147.8, 145.1, 142.2, 141.5 (br), 141.2, 139.0, 135.8, 129.8, 128.6, 127.9, 126.8, 126.5, 125.9, 125.1, 123.8, 123.6, 123.5, 23.6, 21.4. ^{11}B NMR (160 MHz, CD_2Cl_2, ppm): δ 64 (s, br). MS (EI^+) m/z: 658 $[M]^+$. Anal. Calcd (%) for $C_{44}H_{40}BNS_2$: C, 80.35; H, 6.13; N, 2.13; S, 9.75. Found: C, 80.65; H, 6.15; N, 1.94; S, 9.72.

Tpa–Th–Th–B(Pfp)$_2$ (2). THF (1 mL) and $C_2H_4Br_2$ (4 drops) were added sequentially to magnesium turnings (1.03 g, 42.9 mmol) at r.t., and the resulting mixture was stirred for 5 min. A solution of Pfp–Br (1.50 g, 4.29 mmol) in THF (4.3 mL) was prepared. A portion (0.4 mL) of the Pfp–Br solution was added at r.t. to the magnesium turnings, and then the mixture was heated to 50 °C before the remaining Pfp–Br solution was added dropwise. After addition, the reaction mixture was heated at 60 °C for 20 min, before it was cooled to r.t. and the solution was transferred to another flask by syringe to leave the excess Mg as a solid residue. BF_3•OEt_2 (0.21 mL, 1.67 mmol) was added dropwise to the prepared Grignard reagent at 0 °C (ice bath). The reaction mixture was heated at 60 °C for 15 min and then cooled to r.t. After the addition of hexane (10 mL), the mixture was filtered, and the filtrate was evaporated under vacuum to give a viscous oil. As-prepared $(Pfp)_2BF$ was dissolved in THF (3 mL) and used without further purification. n-BuLi (1.6 M in hexane, 0.45 mL, 0.72 mmol) was added to a THF (5 mL) solution of Tpa–Th–Th (295 mg, 0.72 mmol) at –78 °C, and the mixture was stirred at this temperature for 1 h. The prepared lithium reagent was transferred to the prepared $(Pfp)_2BF$ solution (0 °C) by cannula. The obtained mixture was warmed to r.t. and stirred overnight. The solvent was removed under vacuum, and the residue was purified by column chromatography (silica gel, 4:1 hexane/CH_2Cl_2) and subsequent precipitation from CH_2Cl_2 by addition of methanol to provide compound **2** as a yellow solid (300 mg, 43% based on Tpa–Th–Th). ^{1}H NMR (500 MHz, CD_2Cl_2, ppm): δ 7.51 (d, J = 4 Hz, 1 H), 7.48 (d, J = 9 Hz, 2 H), 7.41 (d, J = 4 Hz, 1 H), 7.33 (d, J = 4 Hz, 1 H), 7.30–7.27 (m, 4 H), 7.20 (d, J = 4 Hz, 1 H), 7.14 (s, 4 H), 7.13–7.11 (m, 4 H), 7.08–7.04 (m, 4 H), 2.31 (s, 12 H). $^{13}C\{^1H\}$ NMR (126 MHz, CD_2Cl_2, ppm): δ 152.1, 148.3, 147.7, 147.4 (br), 145.8, 145.7 (m, CF), 145.2 (br), 143.7 (m, CF), 143.7, 141.7 (br), 141.7 (m, CF), 139.6 (m, CF), 138.3 (dm, CF), 135.3, 129.8, 129.2, 127.7, 127.2, 127.1, 126.8, 126.2, 125.2, 123.8, 123.6, 123.5, 116.5 (m), 23.9. $^{19}F\{^1H\}$ NMR (188 MHz, CD_2Cl_2, ppm): δ –143.5 (dd, J = 23, 8 Hz, 4 F), –156.9 (t, J = 21 Hz, 2 F), –163.2 to –163.5 (m, 4 F). ^{11}B NMR (160 MHz, CD_2Cl_2, ppm): δ 65 (s, br). MS (EI^+) m/z: 962 $[M]^+$. Anal. Calcd (%) for $C_{54}H_{34}BF_{10}NS_2$: C, 67.44; H, 3.56; N, 1.46; S, 6.76. Found: C, 67.71; H, 3.20; N, 1.56; S, 6.67.

Tpa–Th–Th–B(Tfp)$_2$ (3). THF (1 mL) and $C_2H_4Br_2$ (4 drops) were added sequentially to magnesium turnings (909 mg, 37.9 mmol) at r.t., and the resulting mixture was stirred for 5 min. A solution of Tfp–Br (1.50 g, 3.79 mmol) in THF (5.70 mL) was prepared. A portion (0.5 mL) of the Tfp–Br solution was added at r.t. to the magnesium turnings, and then the mixture was heated to 50 °C before the remaining solution was added dropwise. After addition, the reaction mixture was heated at 60 °C for 30 min, before it was cooled to r.t. and the solution was transferred to another flask by syringe to leave the excess Mg as a solid residue. BF_3•OEt_2 (0.24 mL, 1.91 mmol) was added dropwise to the prepared Grignard reagent at 0 °C (ice bath). The mixture was heated at 60 °C for 1 h, and then cooled to r.t. Hexane (10 mL) was added to the solution, the mixture was filtered and the filtrate was evaporated under vacuum to give a viscous oil. As-prepared $(Tfp)_2BF$ was dissolved in THF (5.5 mL) without further purification. n-BuLi (1.6 M in hexane, 0.18 mL, 0.29 mmol) was added to a THF (2 mL) solution of Tpa–Th–Th (120 mg, 0.29 mmol) at –78 °C, and the mixture was stirred at this temperature for 1 h. To this lithium reagent, a portion of the prepared $(Tfp)_2BF$ solution (2 mL) was added. The mixture was warmed to r.t. and stirred overnight. The solvent was removed under vacuum, and the residue was purified by column chromatography (silica gel, 3:1 hexane/CH_2Cl_2) and subsequent precipitation from CH_2Cl_2 by addition of methanol to provide compound **3** as a yellow solid (198 mg, 65% based on Tpa–Th–Th). ^{1}H NMR (500 MHz, CD_2Cl_2, ppm): δ 8.14 (s, 4 H), 7.89 (s, 2 H), 7.49–7.46 (m, 3 H), 7.41 (d, J = 4 Hz, 1 H), 7.35 (s, 4 H), 7.31(d, J = 4 Hz, 1 H), 7.30–7.27 (m, 4 H), 7.20 (d, J = 4 Hz, 1 H), 7.12–7.10 (m, 4 H), 7.08–7.03 (m, 4 H), 2.34 (s, 12 H). $^{13}C\{^1H\}$ NMR (126 MHz, THF-d_8, ppm): δ 152.7, 149.0, 148.4, 148.2 (br), 146.3, 145.4 (br), 144.5, 143.8, 142.8 (br), 139.4, 135.7, 132.7 (q, $^2J_{CF}$ = 33 Hz), 130.2, 128.4, 128.2 (m), 127.7, 127.2, 127.1, 126.6, 125.6, 124.3, 124.2 (q, $^1J_{CF}$ = 274 Hz), 124.2, 124.1, 121.7 (m), 24.0. $^{19}F\{^1H\}$ NMR (188 MHz, CD_2Cl_2, ppm): δ –63.1 (s, 12 F). ^{11}B NMR (160 MHz, CD_2Cl_2, ppm): *ca.* 66 (weak and broad). MS (EI^+) m/z: 1054 $[M]^+$. Anal. Calcd (%) for $C_{58}H_{40}BF_{12}NS_2$: C, 66.10; H, 3.83; N, 1.33; S, 6.09. Found: C, 66.42; H, 3.75; N, 1.57; S, 6.04.

Tpa–Th–Th–B(FMes)$_2$ (4). n-BuLi (2.5 M in hexane, 0.16 mL, 0.40 mmol) was added to a THF (4 mL) solution of Tpa–Th–Th (150 mg, 0.37 mmol) at –78 °C, and then the mixture was slowly warmed to –25 °C during 1 h. After the solvent was removed under vacuum, toluene (2 mL) was added to the residue at *ca.* –25 °C. A toluene (5 mL) solution of $(FMes)_2BF$ (220 mg, 0.37 mmol) was added to the prepared lithium reagent, the reaction mixture was warmed to r.t. and stirred overnight. The solvent was removed under vacuum, and the residue was purified by column chromatography (silica gel, 4:1 hexane/CH_2Cl_2) and subsequent crystallization from hexane at –30 °C to provide compound **4** as a red solid (40 mg, 11%). ^{1}H NMR (500 MHz, THF-d_8, ppm): δ 8.44 (s, 4 H), 7.52 (d, J = 9 Hz, 2 H), 7.48 (d, J = 4 Hz, 2 H), 7.44 (d, J = 4 Hz, 1 H), 7.34 (d, J = 4 Hz, 1 H), 7.32 (d, J = 4 Hz, 1 H), 7.27–7.24 (m, 4 H), 7.09–7.07 (m, 4 H), 7.04–7.02 (m, 4 H). $^{13}C\{^1H\}$ NMR (126 MHz, THF-d_8, ppm): δ 154.8, 149.2, 148.3, 147.7, 146.4, 134.6, 133.9, 133.6, 130.2, 129.1, 128.1, 127.3, 126.5, 125.7, 124.9, 124.5, 124.3, 123.9, 122.7. $^{19}F\{^1H\}$ NMR (188 MHz, CD_2Cl_2, r.t., ppm): δ –50.4 (s, br, 3 F), –52.1 (s, br, 3 F), –56.5 (s, br, 6 F), –63.4 (s, 6 F). $^{19}F\{^1H\}$ NMR (188 MHz, CD_2Cl_2, 223 K, ppm): δ –50.0 (q, J = 13 Hz, 3 F), –51.8 (q, J = 11 Hz, 3 F), –56.0 (q, J = 11 Hz, 3 F), –56.4 (q, J = 13 Hz, 3 F), –62.8 (s, 3 F), –62.9 (s, 3 F). ^{11}B NMR (160 MHz, THF-d_8, ppm): not observed. MS (EI^+) m/z: 981 $[M]^+$. Anal. Calcd (%) for $C_{44}H_{22}BF_{18}NS_2$: C, 53.84; H, 2.26; N, 1.43; S, 6.53. Found: C, 54.34; H, 2.44; N, 1.66; S, 6.33.

Tmjul–Th–Th–B(Pfp)$_2$ (5). n-BuLi (1.6 M in hexane, 0.63 mL, 1.01 mmol) was added to a THF (2.3 mL) solution of Tmjul–Th–Th (375 mg, 0.95 mmol) at –78 °C, and the mixture was stirred at this temperature for 1 h. The prepared lithium reagent was transferred to a THF solution of $(Pfp)_2BF$ at 0 °C, which was prepared using the same method and in the same amount as that used in the synthesis of **2**. The mixture was warmed to r.t. and stirred overnight. The solvent was removed under vacuum, and the residue was purified by column chromatography (silica gel, 3:1 hexane/CH_2Cl_2) and subsequent precipitation from CH_2Cl_2 by addition of methanol to provide compound **5** as a red solid (430 mg, 48% based on Tmjul–Th–Th). ^{1}H NMR (500 MHz, THF-d_8, ppm): δ 7.52 (d, J = 4 Hz, 1 H), 7.46 (d, J = 4 Hz, 1 H), 7.38 (d, J = 4 Hz, 1 H), 7.31 (s, 2 H), 7.19 (s, 4 H), 7.15(d, J = 4 Hz, 1 H), 3.22 (t, J = 6 Hz, 4 H), 2.32 (s, 12 H), 1.76 (t, J = 6 Hz, 4 H), 1.30 (s, 12 H). $^{13}C\{^1H\}$ NMR (126 MHz, THF-d_8, ppm): δ 154.0, 149.2, 147.0 (br), 145.8 (br), 145.6 (dm, CF), 144.5, 142.3–142.1 (m, 2 C), 141.7, 140.2 (br, CF), 138.8 (dm, CF), 133.4, 131.3, 129.7, 127.8, 127.7, 126.0, 122.3, 121.9, 121.7, 117.2 (m), 47.4, 37.6, 33.0, 31.3, 23.9. $^{19}F\{^1H\}$ NMR (188 MHz, CD_2Cl_2, ppm): δ –143.5 (dd, J = 23, 8 Hz, 4 F), –157.0 (t, J = 21 Hz, 2 F), –163.2 to –163.5 (m, 4 F). ^{11}B NMR (160 MHz, THF-d_8, ppm): *ca.* 65 (weak and broad). MS (EI^+) m/z: 946 $[M]^+$. Anal. Calcd (%) for $C_{52}H_{42}BF_{10}NS_2$: C, 66.03; H, 4.48; N, 1.48; S, 6.78. Found: C, 66.39; H, 4.25; N, 1.49; S, 6.54.

Tmjul–Th–Th–B(Tfp)$_2$ (6). *n*-BuLi (1.6 M in hexane, 0.40 ml, 0.64 mmol) was added to a THF (1.5 mL) solution of Tmjul–Th–Th (250 mg, 0.64 mmol) at –78 °C, and the mixture was stirred at this temperature for 1 h. A solution of (Tfp)$_2$BF in THF (3.5 mL), prepared in the same batch as that used in the synthesis of **3**, was added to the to the lithium reagent. The mixture was warmed to r.t. and stirred overnight. The solvent was removed under vacuum, and the residue was purified by column chromatography (silica gel, 3:1 hexane/CH_2Cl_2) and subsequent precipitation from CH_2Cl_2 by addition of methanol to provide compound **6** as a red solid (330 mg, 50% based on Tmjul–Th–Th). ^{1}H NMR (500 MHz, CD_2Cl_2, ppm): δ 8.15 (s, 4 H), 7.90 (s, 2 H), 7.47 (d, J = 4 Hz, 1 H), 7.38 (d, J = 4 Hz, 1 H), 7.36 (s, 4 H), 7.29 (d, J = 4 Hz, 1 H), 7.27 (s, 2 H), 7.08 (s, br, 1 H), 3.21 (s, br, 4 H), 2.35 (s, 12 H), 1.76 (t, J = 6 Hz, 4 H), 1.30 (s, 12 H). ^{13}C{^{1}H} NMR (126 MHz, THF-d_8, ppm): δ 153.7, 149.1, 147.4 (br), 145.4 (br), 144.6, 144.0, 142.8 (br), 141.7, 139.3, 133.4, 132.7 (q, $^2J_{CF}$ = 33 Hz), 131.3, 128.2 (m), 127.6, 127.1, 125.9, 124.7 (q, $^1J_{CF}$ = 273 Hz), 122.3, 121.9, 121.7, 121.6 (m), 47.4, 37.6, 33.0, 31.3, 24.0. ^{19}F{^{1}H} NMR (188 MHz, CD_2Cl_2, ppm): δ –63.2 (s, 12 F). ^{11}B NMR (160 MHz, THF-d_8, ppm): *ca.* 65 (weak and broad). MS (EI$^+$) *m/z*: 1038 [M]$^+$. Anal. Calcd (%) for $C_{56}H_{48}BF_{12}NS_2$: C, 64.80; H, 4.66; N, 1.35; S, 6.18. Found: C, 65.12; H, 4.84; N, 1.55; S, 6.09.

Acknowledgements

We are grateful for generous financial support by the Bavarian State Ministry of Science, Research, and the Arts for the Collaborative Research Network “Solar Technologies go Hybrid”. Z. Z. and R. M. E. thank the Alexander von Humboldt Foundation for Postdoctoral Research Fellowships. The authors thank Dr. Stefan Wagner for mass spectrometry measurements, Dr. Rüdiger Bertermann for NMR measurements, Dr. Ivo Krummenacher for help with electrochemical measurements, and Prof. Dr. Christoph Lambert for access to the FLS980 spectrofluorimeter.

Keywords: Boron • Fluorescence • Charge transfer • Photophysics • Near infrared

[1] For reviews, see: a) C. D. Entwistle, T. B. Marder, *Angew. Chem. Int. Ed.* **2002**, *41*, 2927–2931; b) C. D. Entwistle, T. B. Marder, *Chem. Mater.* **2004**, *16*, 4574–4585; c) S. Yamaguchi, A. Wakamiya, *Pure Appl. Chem.* **2006**, *78*, 1413–1424; d) Z. M. Hudson, S. Wang, *Acc. Chem. Res.* **2009**, *42*, 1584–1596; e) Z. M. Hudson, S. Wang, *Dalton Trans.* **2011**, *40*, 7805–7816; f) F. Jäkle, *Coord. Chem. Rev.* **2006**, *250*, 1107–1121; g) F. Jäkle, *Chem. Rev.* **2010**, *110*, 3985–4022; h) C. R. Wade, A. E. J. Broomsgrove, S. Aldridge, F. P. Gabbaï, *Chem. Rev.* **2010**, *110*, 3958–3984; i) T. W. Hudnall, C.-W. Chiu, F. P. Gabbaï, *Acc. Chem. Res.* **2009**, *42*, 388–397; j) M. J. D. Bosdet, W. E. Piers, *Can. J. Chem*. **2009**, *87*, 8–29; k) M. Elbing, G. C. Bazan, *Angew. Chem. Int. Ed.* **2008**, *47*, 834–838; l) N. Matsumi, Y. Chujo, *Polym. J.* **2008**, *40*, 77–89; m) Y. Shirota, *J. Mater. Chem.* **2000**, *10*, 1–25; n) Y. Shirota, H. Kageyama, *Chem. Rev.* **2007**, *107*, 953–1010.

[2] a) L. Weber, V. Werner, M. A. Fox, T. B. Marder, S. Schwedler, A. Brockhinke, H.-G. Stammler, B. Neumann, *Dalton Trans*. **2009**, 2823–2831; b) H. Braunschweig, T. Herbst, D. Rais, S. Ghosh, T. Kupfer, K. Radacki, A. G. Crawford, R. M. Ward, T. B. Marder, I. Fernández, G. Frenking, *J. Am. Chem. Soc*. **2009**, *131*, 8989–8999; c) L. Weber, D. Eickhoff, T. B. Marder, M. A. Fox, P. J. Low, A. D. Dwyer, D. J. Tozer, S. Schwedler, A. Brockhinke, H. G. Stammler, B. Neumann, *Chem. Eur. J.* **2012**, *18*, 1369–1382; d) C. D. Entwistle, J. C. Collings, A. Steffen, L.-O. Pålsson, A. Beeby, D. Albesa-Jove, J. M. Burke, A. S. Batsanov, J. A. K. Howard, J. A. Mosely, S.-Y. Poon, W.-Y. Wong, F. Ibersiene, S. Fathallah, A. Boucekkine, J.-F. Halet, T. B. Marder, *J. Mater. Chem.* **2009**, *19*, 7532–7544; e) L. Ji, R. M. Edkins, L. J. Sewell, A. Beeby, A. S. Batsanov, K. Fucke, M. Drafz, J. A. K. Howard, O. Moutounet, F. Ibersiene, A. Boucekkine, E. Furet, Z. Liu, J.-F. Halet, C. Katan, T. B. Marder, *Chem. Eur. J.* **2014**, *20*, 13618–13635; f) G. Zhou, C.-L. Ho, W.-Y. Wong, Q. Wang, D. Ma, L. Wang, Z. Lin, T. B. Marder, A. Beeby, *Adv. Funct. Mater.* **2008**, *18*, 499–511; g) A. G. Crawford, Z. Liu, I. A. I. Mkhalid, M. -H. Thibault, N. Schwarz, G. Alcaraz, A. Steffen, J. C. Collings, A. S. Batsanov, J. A. K. Howard, T. B. Marder, *Chem. Eur. J.* **2012**, *18*, 5022–5035.

[3] a) A. Wakamiya, T. Ide, S. Yamaguchi, *J. Am. Chem. Soc.* **2005**, *127*, 14859–14866; b) S. Yamaguchi, S. Akiyama, K. Tamao, *J. Am. Chem. Soc.* **2001**, *123*, 11372–11375; c) S. Yamaguchi, T. Shirasaka, S. Akiyama, K. Tamao, *J. Am. Chem. Soc.* **2002**, *124*, 8816–8817; d) Y. Kubo, M. Yamamoto, M. Ikeda, M. Takeuchi, S. Shinkai, S. Yamaguchi, K. Tamao, *Angew. Chem. Int. Ed.* **2003**, *42*, 2036–2040; e) S. Yamaguchi, S. Akiyama, K. Tamao, *J. Am. Chem. Soc.* **2000**, *122*, 6335–6336; f) C.-H. Zhao, E. Sakuda, A. Wakamiya, S. Yamaguchi, *Chem. Eur. J.* **2009**, *15*, 10603–10612; g) A. Shuto, T. Kushida, T. Fukushima, H. Kaji, S. Yamaguchi, *Org. Lett.* **2013**, *15*, 6234–6237; h) C.-H. Zhao, A. Wakamiya, S. Yamaguchi, *Macromolecules* **2007**, *40*, 3898–3900; i) A. Wakamiya, K. Mori, S. Yamaguchi, *Angew. Chem. Int. Ed*. **2007**, *46*, 4273–4276; j) C.-H. Zhao, A. Wakamiya, Y. Inukai, S. Yamaguchi, *J. Am. Chem. Soc.* **2006**, *128*, 15934–15935; k) Z. Zhou, A. Wakamiya, T. Kushida, S. Yamaguchi, *J. Am. Chem. Soc.* **2012**, *134*, 4529–4532; l) S. Saito, K. Matsuo, S. Yamaguchi, *J. Am. Chem. Soc.* **2012**, *134*, 9130–9133; m) C. Dou, S. Saito, K. Matsuo, I. Hisaki, S. Yamaguchi, *Angew. Chem. Int. Ed.* **2012**, *51*, 12206–12210; n) T. Kushida, C. Camacho, A. Shuto, S. Irle, M. Muramatsu, T. Katayama, S. Ito, Y. Nagasawa, H. Miyasaka, E. Sakuda, N. Kitamura, Z. Zhou, A. Wakamiya, S. Yamaguchi, *Chem. Sci*. **2014**, *5*, 1296–1304; o) A. Shuto, T. Kushida, T. Fukushima, H. Kaji, S. Yamaguchi, *Org. Lett.* **2013**, *15*, 6234–6237; p) T. Taniguchi, J. Wang, S. Irle, S. Yamaguchi, *Dalton Trans.* **2013**, *42*, 620–624; q) J. Wang, Y. Wang, T. Taniguchi, S. Yamaguchi, S. Irle, *J. Phys. Chem. A* **2012**, *116*, 1151–1158; r) T. Kushida, S. Yamaguchi, *Organometallics* **2013**, *32*, 6654–6657.

[4] a) M. Varlan, B. A. Blight, S. Wang, *Chem. Commun.* **2012**, *48*, 12059–12061; b) Y. Sun, N. Ross, S.-B. Zhao, K. Huszarik, W.-L. Jia, R.-Y. Wang, D. Macartney, S. Wang, *J. Am. Chem. Soc.* **2007**, *129*, 7510–7511; c) X. Y. Liu, D. R. Bai, S. Wang, *Angew. Chem. Int. Ed.* **2006**, *45*, 5475–5478; d) Z. M. Hudson, C. Sun, M. G. Helander, H. Amarne, Z.-H. Lu, S. Wang, *Adv. Funct. Mater.* **2010**, *20*, 3426–3439; e) Z. Wang, M. G. Helander, Z. M. Hudson, J. Qiu, S. Wang, Z.-H. Lu, *Appl. Phys. Lett.* **2011**, *98*, 213301–213303; f) Y. Rao, D. Schoenmakers, Y.-L. Chang, J. Lu, Z.-H. Lu, Y. Kang, S. Wang, *Chem. Eur. J.* **2012**, *18*, 11306–11316; g) C. Sun, Z. M. Hudson, M. G. Helander, Z.-H. Lu, S. Wang, *Organometallics* **2011**, *30*, 5552–5555; h) Z. M. Hudson, C. Sun, M. G. Helander, Y.-L. Chang, Z.-H. Lu, S. Wang, *J. Am. Chem. Soc.* **2012**, *134*, 13930–13933; i) S.-B. Ko, J.-S. Lu, Y. Kang, S. Wang, *Organometallics* **2013**, *32*, 599–607; j) W.-L. Jia, D. Song, S. Wang, *J. Org. Chem.* **2003**, *68*, 701–705.

[5] a) F. Pammer, F. Jäkle, *Chem. Sci.* **2012**, *3*, 2598–2606; b) P. Chen, F. Jäkle, *J. Am. Chem. Soc.* **2011**, *133*, 20142–20145; c) H. Li, R. A. Lalancette, F. Jäkle, *Chem. Commun.* **2011**, *47*, 9378–9380; d) P. Chen, R. A. Lalancette, F. Jäkle, *Angew. Chem. Int. Ed.* **2012**, *51*, 7994–7998; e) F. Cheng, E. M. Bonder, F. Jäkle, *J. Am. Chem. Soc.* **2013**, *135*, 17286–17289; f) P. Chen, R. A. Lalancette, F. Jäkle, *J. Am. Chem. Soc.* **2011**, *133*, 8802–8805; g) Y. Qin, G. Cheng, O. Achara, K. Parab, F. Jäkle, *Macromolecules* **2004**, *37*, 7123–7131; h) X. Yin, J. Chen, R. A. Lalancette, T. B. Marder, F. Jäkle, *Angew. Chem. Int. Ed.* **2014**, *53*, 9761–9765; i) A. Lorbach, M. Bolte, H. Li, H.-W. Lerner, M. C. Holthausen, F. Jäkle, M. Wagner, *Angew. Chem. Int. Ed.* **2009**, *48*, 4584–4588; j) E. Januszewski, M. Bolte, H.-W. Lerner, M. Wagner, *Organometallics* **2012**, *31*, 8420–8425; k) E. Januszewski, A. Lorbach, R. Grewal, M. Bolte, J. W. Bats, H.-W. Lerner, M. Wagner, *Chem. Eur. J.* **2011**, *17*, 12696 – 12705; l) C. Reus, S. Weidlich, M. Bolte, H.-W. Lerner, M. Wagner, *J. Am. Chem. Soc.* **2013**, *135*, 12892−12907; m) Y. Qin, I. Kiburu, S. Shah, F. Jäkle, *Org. Lett.* **2006**, *8*, 5227–5230.

[6] a) H. Zhao, J. H. Reibenspies, F. P. Gabbaï, *Dalton Trans.* **2013**, *42*, 608–610; b) T. W. Hudnall, F. P. Gabbaï, *J. Am. Chem. Soc.* **2007**, *129*, 11978–11986; c) C.-W. Chiu, F. P. Gabbaï, *Dalton Trans.* **2008**, 814–817; d) Y. Kim, F. P. Gabbaï, *J. Am. Chem. Soc.* **2009**, *131*, 3363–3369; e) H. Zhao, F. P. Gabbaï, *Nature Chem.* **2010**, *2*, 984–990; f) H. Zhao, F. P. Gabbaï, *Organometallics* **2012**, *31*, 2327−2335.

[7] a) N. Matsumi, K. Naka, Y. Chujo, *J. Am. Chem. Soc.* **1998**, *120*, 5112–5113; b) D. Cao, Z. Liu, G. Li, G. Liu, G. Zhang, *J. Mol. Struct.* **2008**, *874*, 46–50; c) Z. Liu, Q. Fang, D. Cao, D. Wang, G. Xu, *Org. Lett.* **2004**, *6*, 2933–2936; d) L. Ji, Q. Fang, M.-S. Yuan, Z.-Q. Liu, Y.-X. Shen, H.-F. Chen, *Org. Lett.* **2010**, *12*, 5192–5195; e) M. Lequan, R. M. Lequan, K. Chane-Ching, A.-C. Callier, M. Barzoukas, A. Fort, *Adv. Mater. Opt. Electron.* **1992**, *1*, 243–247; f) T. Noda, H. Ogawa, Y. Shirota, *Adv. Mater.* **1999**, *11*, 283–285; g) G. J. Zhou, Q. Wang, X. Z. Wang, C.-L. Ho, W.-Y.

Wong, D. G. Ma, L. X. Wang, Z. Y. Lin, *J. Mater. Chem.* **2010**, *20*, 7472–7484; h) A. Pron, M. Baumgarten, K. Müllen, *Org. Lett.* **2010**, *12*, 4236–4239; i) M. M. Olmstead, P. P. Power, *J. Am. Chem. Soc.* **1986**, *108*, 4235–4236; (j) M. J. D. Bosdet, W. E. Piers, T. S. Sorensen, M. Parvez, *Angew. Chem. Int. Ed.* **2007**, *46*, 4940–4943; (k) B. Neue, J. F. Araneda, W. E. Piers, M. Parvez, *Angew. Chem. Int. Ed.* **2013**, *52*, 9966–9969.

[8] a) D.-X. Cao, Z.-Q. Liu, Q. Fang,. G.-B. Xu, G. Xue, G.-Q. Liu, W.-T. Yu, *J. Organomet. Chem.* **2004**, *689*, 2201–2206; b) R. Stahl, C. Lambert, C. Kaiser, R. Wortmann, R. Jakober, *Chem. Eur. J.* **2006**, *12*, 2358–2370; c) U. Megerle, F. Selmaier, C. Lambert, E. Riedle, S. Lochbrunner, *Phys. Chem. Chem. Phys.* **2008**, *10*, 6245–6251; d) W. Zhao, X. Zhuang, D. Wu, F. Zhang, D. Gehrig, F. Laquai, X. Feng, *J. Mater. Chem. A* **2013**, *1*, 13878–13884; e) D. Reitzenstein, C. Lambert, *Macromolecules* **2009**, *42*, 773–782; f) P. Sudhakar, S. Mukherjee, P. Thilagar, *Organometallics* **2013**, *32*, 3129−3133; f) J. C. Doty, B. Babb, P. J. Grisdale, M. Glogowski, J. L. R. Williams, *J. Organomet. Chem.* **1972**, *38*, 229–236.

[9] a) Z. Yuan, N. J. Taylor, T. B. Marder, I. D. Williams, S. K. Kurtz, L.-T. Cheng, *J. Chem. Soc.*, *Chem. Commun.* **1990**, 1489–1492; b) Z. Yuan, N. J. Taylor, T. B. Marder, I. D. Williams, S. K. Kurtz, L.-T. Cheng, in *Organic Materials for Non-linear Optics II*, (Eds.: R. A. Hann, D. Bloor), Royal Society of Chemistry, Cambridge, **1991**, pp 190–196; c) Z. Yuan, N. J. Taylor, Y. Sun, T. B. Marder, I. D. Williams, L.-T. Cheng, *J. Organomet. Chem.* **1993**, *449*, 27–37; d) Z. Yuan, N. J. Taylor, R. Ramachandran, T. B. Marder, *Appl. Organomet. Chem.* **1996**, *10*, 305–316; e) Z. Yuan, J. C. Collings, N. J. Taylor, T. B. Marder, C. Jardin, J.-F. Halet, *J. Solid State Chem.* **2000**, *154*, 5–12; f) Z. Yuan, C. D. Entwistle, J. C. Collings, D. Albesa-Jové, A. S. Batsanov, J. A. K. Howard, N. J. Taylor, H. M. Kaiser, D. E. Kaufmann, S.-Y. Poon, W.-Y. Wong, C. Jardin, S. Fathallah, A. Boucekkine, J.-F. Halet, T. B. Marder, *Chem. Eur. J.* **2006**, *12*, 2758–2771; g) M. Charlot, L. Porrès, C. D. Entwistle, A. Beeby, T. B. Marder, M. Blanchard-Desce, *Phys. Chem. Chem. Phys.* **2005**, *7*, 600–606; h) L. Porrès, M. Charlot, C. D. Entwistle, A. Beeby, T. B. Marder, M. Blanchard-Desce, *Proc. SPIE* **2005**, *92*, 5934–5936; i) J. C. Collings, S.-Y. Poon, C. Le Droumaguet, M. Charlot, C. Katan, L.-O. Pålsson, A. Beeby, J. A. Mosely, H. M. Kaiser, D. Kaufmann, W.-Y. Wong, M. Blanchard-Desce, T. B. Marder, *Chem. Eur. J.* **2009**, *15*, 198–208; j) N. S. Makarov, S. Mukhopadhyay, K. Yesudas, J.-L. Brédas, J. W. Perry, A. Pron, M. Kivala, K. Müllen, *J. Phys. Chem. A* **2012**, *116*, 3781–3793; k) M. Lequan, R. M. Lequan, K. C. Ching, *J. Mater. Chem.* **1991**, *1*, 997–999; l) M. Lequan, R. M. Lequan, K. C. Ching, M. Barzoukas, A. Fort, H. Lahoucine, B. Bravic, D. Chasseau, J. Gaultier, *J. Mater. Chem.* **1992**, *2*, 719–725; m) C. Branger, M. Lequan, R. M. Lequan, M. Barzoukas, A. Fort, *J. Mater. Chem.* **1996**, *6*, 555–558; n) Z. Liu, Q. Fang, D. Wang, G. Xue, W. Yu, Z. Shao, M. Jiang, *Chem. Commun.* **2002**, 2900–2901; o) D. Cao, Z. Liu, Q. Fang, G. Xu, G. Liu, W. Yu, *J. Organomet. Chem.* **2004**, *689*, 2201–2206; p) Z. Liu, Q. Fang, D. Wang, D. Cao, G. Xue, W. Yu, H. Lei, *Chem. Eur. J.* **2003**, *9*, 5074–5084.

[10] a) Y. Shirota, M. Kinoshita, T. Noda, K. Okumoto, T. Ohara, *J. Am. Chem. Soc.* **2000**, *122*, 11021–11022; b) H. Doi, M. Kinoshita, K. Okumoto, Y. Shirota, *Chem. Mater.* **2003**, *15*, 1080–1089; c) F. Li, W. Jia, S. Wang, Y. Zhao, Z.-H. Lu, *J. Appl. Phys.* **2008**, *103*, 034509/1–034509/6; d) W. L. Jia, M. J. Moran, Y. Y. Yuan, Z. H. Lu, S. Wang, *J. Mater. Chem.* **2005**, *15*, 3326–3333; e) W.-L. Jia, D.-R. Bai, T. McCormick, Q.-D. Liu, M. Motala, R.-Y. Wang, C. Seward, Y. Tao, S. Wang, *Chem. Eur. J.* **2004**, *10*, 994–1006; f) Z. M. Hudson, C. Sun, M. G. Helander, H. Amarne, Z. H. Lu, S. Wang, *Adv. Funct. Mater.* **2010**, *20*, 3426–3439; g) Z. M. Hudson, M. G. Helander, Z.-H. Lu, S. Wang, *Chem. Commun.* **2011**, *47*, 755－757; h) W. Zhang, Z. He, Y. Wang, S. Zhao, *Synth. Met.* **2011**, *161*, 2323–2328; i) C.-T. Chen, W.-S. Chao, H.-W. Liu, Y. Wei, J.-H. Jou, S. Kumar, *RSC Adv*. **2013**, *3*, 9381–9390; j) H.-G. Jang, B. S. Kim, J. Y. Lee, S.-H. Wang, *Dalton Trans.* **2014**, *43*, 7712–7715; k) L. Y. Zou, A. M. Ren, J. K. Feng, Y. L. Liu, X. Q. Ran, C. C. Sun, *J. Phys. Chem. A* **2008**, *112*, 12172–12178.

[11] a) D. Cao, Z. Liu, G. Zhang, G. Li, *Dyes Pigments* **2009**, *81*, 193–196; b) Z.-Q. Liu, M. Shi, F.-Y. Li, Q. Fang, Z.-H. Chen, T. Yi, C.-H. Huang, *Org. Lett.* **2005**, *7*, 5481–5484; c) D. Cao, Z. Liu, G. Li. *Sensors, Actuators B* **2008**, *133*, 489–492; d) C. A. Swamy P, P. Thilagar, *Inorg. Chem.* **2014**, *53*, 2776–2786; e) Y. Sun, S. Wang, *Inorg. Chem.* **2009**, *48*, 3755–3767; f) M.-S. Yuan, Z.-Q. Liu, Q. Fang, *J. Org. Chem.* **2007**, *72*, 7915–7922.

[12] a) Y. J. Zhang, Y. X. Jin, R. Bai, Z.W. Yu, B. Hu, M. Ouyang, J. W. Sun, C. H. Yu, J. L. Liu, C. Zhang, *J. Photochem. Photobiol. A-Chem.* **2012**, *227*, 59–64; b) C. Karunakaran, J. Jayabharathi, M. V. Perumal, V. Thanikachalam, P. K. Thakur, *J. Phys. Org. Chem.* **2013**, *26*, 386–406; c) U. Purushotham, G. N. Sastry, *Phys. Chem. Chem. Phys.* **2013**, *15*, 5039–5048.

[13] a) A. Wakamiya, K. Mishima, K. Ekawa, S, Yamaguchi, *Chem. Commun.* **2008**, 579–581; b) T. Agou, J. Kobayashi, T. Kawashima, *Chem. Eur. J.* **2007**, *13*, 8051–8060; c) T. Agou, T. Kojima, J. Kobayashi, T. Kawashima, *Org. Lett.* **2009**, *11*, 3534–3537.

[14] a) A. Sundararaman, K. Venkatasubbaiah, M. Victor, L. N. Zakharov, A. L. Rheingold, F. Jäkle, *J. Am. Chem. Soc.* **2006**, *128*, 16554–16565; b) A. Sundararaman, R. Varughese, H. Li, L. N. Zakharov, A. L. Rheingold, F. Jäkle, *Organometallics* **2007**, *26*, 6126–6131; c) H. Braunschweig, A. Damme, J. O. C. Jimenez-Halla, C. Hörl, I. Krummenacher, T. Kupfer, L. Mailänder, K. Radacki, *J. Am. Chem. Soc.* **2012**, *134*, 20169–20177; d) A. E. Ashley, T. J. Herrington, G. G. Wildgoose, H. Zaher, A. L. Thompson, N. H. Rees, T. Krämer, D. O'Hare, *J. Am. Chem. Soc.* **2011**, *133*, 14727–14740; e) M.-G. Ren, Q.-H. Song, *Chem. Commun.* **2012**, *48*, 2970–2972; f) M. Mao, M.-G. Ren, Q.-H. Song, *Chem. Eur. J.* **2012**, *18*, 15512–15522; g) C.-W. Chiu, Y. Kim, F. P. Gabbaï, *J. Am. Chem. Soc.* **2009**, *131*, 60–61.

[15] Z. Zhang, R. M. Edkins, J. Nitsch, K. Fucke, A. Steffen, L. E. Longobardi, D. W. Stephan, C. Lambert, T. B. Marder, *Chem. Sci.* **2014**, DOI: 10.1039/c4sc02410a.

[16] a) Y. J. Chang, T. J. Chow, *Tetrahedron* **2009**, *65*, 4726–4734; b) D. Demeter, V. Jeux, P. Leriche, P. Blanchard, Y. Olivier, J. Cornil, R. Po, J. Roncali, *Adv. Funct. Mater.* **2013**, *23*, 4854–4861.

[17] I. A. I. Mkhalid, J. H. Barnard, T. B. Marder, J. M. Murphy, J. F. Hartwig, *Chem. Rev.* **2010**, *110*, 890–931.

[18] a) G. Wu, F. Kong, J. Li, W. Chen, X. Fang, C. Zhang, Q. Chen, X. Zhang, S. Dai, *Dyes and Pigments* **2013**, *99*, 653–660; b) H. Wang, Z. Lu, S. J. Lord, K. A. Willets, J. A. Bertke, S. D. Bunge, W. E. Moerner, R. J. Twieg, *Tetrahedron* **2007**, *63*, 103–114; c) J. Shao, S. Ji, Xiaolian Li, J. Zhao, F. Zhou, H. Guo, *Eur. J. Org. Chem.* **2011**, 6100–6109.

[19] F. Schlütter, F. Rossel, M. Kivala, V. Enkelmann, J.-P. Gisselbrecht, P. Ruffieux, R. Fasel, K. Müllen, *J. Am. Chem. Soc.* **2013**, *135*, 4550−4557.

[20] S. Lucas, M. Negri, R. Heim, C. Zimmer, R. W. Hartmann, *J. Med. Chem.* **2011**, *54*, 2307–2319.

[21] J. Pommerehne, H. Vestweber, W. Guss, R. F. Mahrt, H. Bässler, M. Porsch, J. Daub, *Adv. Mater.* **1995**, *7*, 551–554.

[22] C.-L. Ho, B. Yao, B. Zhang, K.-L. Wong, W.-Y. Wong, Z. Xie, L. Wang, Z. Lin, *J. Organomet. Chem.* **2013**, *730*, 144–155.

[23] S. K. Sarkar, S. Mukherjee, P. Thilagar, *Inorg. Chem.* **2014**, *53*, 2343−2345.

[24] a) K. Umezawa, Y. Nakamura, H. Makino, D. Citterio, K. Suzuki, *J. Am. Chem. Soc.* **2008**, *130*, 1550–1551; b) R. Yoshii, A. Nagai, K. Tanaka, Y. Chujo, *J. Polym. Sci.*, *Par A*: *Polym. Chem*. **2013**, *51*, 1726–1733.

[25] L. Weber, D. Eickhoff, J. Kahlert, L. Böhling, A. Brockhinke, H.-G. Stammler, B. Neumann, M. A. Fox, *Dalton Trans.* **2012**, *4*, 10328–10346.

[26] a) J. D. Luo, Z. L. Xie, J. W. Y. Lam, L. Cheng, H. Y. Chen, C. F. Qiu, H. S. Kwok, X. W. Zhan, Y. Q. Liu, D. B. Zhu, B. Z. Tang, *Chem. Commun.* **2001**, 1740–1741; b) Q. Wu, T. Zhang, Q. Peng, D. Wang, Z. Shuai, *Phys. Chem. Chem. Phys.* **2014**, *16*, 5545–5552; c) K. Ye, J. Wang, H. Sun, Y. Liu, Z. Mu, F. Li, S. Jiang, J. Zhang, H. Zhang, Y. Wang, C. M. Che, *J. Phys. Chem. B* **2005**, *109*, 8008–8016; d) X. Cheng, D. Li, Z. Zhang, H. Zhang, Y. Wang, *Org. Lett.* **2014**, *16*, 880−883; e) Z. Zhang, Y. Zhang, D. Yao, H. Bi, I. Javed, Y. Fan, H. Zhang, Y. Wang, *Cryst. Growth Des.* **2009**, *9*, 5069−5076.

[27] a) J. Chen, C. C. W. Law, J. W. Y. Lam, Y. Dong, S. M. F. Lo, I. D. Williams, D. Zhu, B. Z. Tang, *Chem. Mater.* **2003**, *15*, 1535**–**1546; b) Y. Hong, J. W. Y. Lam, B. Z. Tang, *Chem. Commun.* **2009**, 4332**–**4353; c) B. K. An, S. K. Kwon, S. D. Jung, S. Y. Park, *J. Am. Chem. Soc.* **2002**, *124*, 14410–14415; d) Z. Q. Xie, B. Yang, F. Li, G. Cheng, L. L. Liu, G. D. Yang, H. Xu, L. Ye, M. Hanif, S. Y. Liu, D. G. Ma, Y. G. Ma, *J. Am. Chem. Soc.* **2005**, *127*, 14152**–**14153.

[28] W. Z. Yuan, S. Chen, J. W. Y. Lam, C. Deng, P. Lu, H. H-Y. Sung, I. D. Williams, H. S. Kwok, Y. Zhang, B. Z. Tang, *Chem. Commun.* **2011**, *47*, 11216–11218.

[29] a) B.-R. Gao, H.-Y. Wang, Y.-W. Hao, L.-M. Fu, H.-H. Fang, Y. Jiang, L. Wang, Q.-D. Chen, H. Xia, L.-Y. Pan, Y.-G. Ma, H.-B Sun, *J. Phys. Chem. B* **2010**, *114*, 128–134; b) R. Hu, E. Lager, A. Aguilar-Aguilar, J. Liu, J. W. Y. Lam, H. H. Y. Sung, I. D. Williams, Y. Zhong, K. S. Wong, E. Peña-Cabrera, B. Z. Tang, *J. Phys. Chem. C* **2009**, *113*, 15845–15853.

[30] S. M. Cornet, K. B. Dillon, C. D. Entwistle, M. A. Fox, A. E. Goeta, H. P. Goodwin, T. B. Marder, A. L. Thompson, *Dalton Trans.* **2003**, 4395–4405.

[31] D.-S. Kim, K. H. Ahn, *J. Org. Chem.* **2008**, *73*, 6831–6834.

[32] P. F. Xia, X. J. Feng, J. Lu, R. Movileanu, Y. Tao, J.-M. Baribeau, M. S. Wong, *J. Phys. Chem. C* **2008**, *112*, 16714–1672.

[33] R. Uson, L. A. Oro, J. A. Cabeza, H. E. Bryndza, M. P. Stepro, *Inorg. Synth*. **1985**, *23*, 126–130.

[34] O. V. Dolomanov, L. J. Bourhis, R. J. Gildea, J. A. K. Howard, H. Puschmann, *J. Appl. Cryst.* **2009**, *42*, 339–341.

[35] Gaussian 09, Revision B.01, M. J. Frisch, G. W. Trucks, H. B. Schlegel, G. E. Scuseria, M. A. Robb, J. R. Cheeseman, G. Scalmani, V. Barone, B. Mennucci, G. A. Petersson, H. Nakatsuji, M. Caricato, X. Li, H. P. Hratchian, A. F. Izmaylov, J. Bloino, G. Zheng, J. L. Sonnenberg, M. Hada, M. Ehara, K. Toyota, R. Fukuda, J. Hasegawa, M. Ishida, T. Nakajima, Y. Honda, O. Kitao, H. Nakai, T. Vreven, J. A. Montgomery, Jr., J. E. Peralta, F. Ogliaro, M. Bearpark, J. J. Heyd, E. Brothers, K. N. Kudin, V. N. Staroverov, T. Keith, R. Kobayashi, J. Normand, K. Raghavachari, A. Rendell, J. C. Burant, S. S. Iyengar, J. Tomasi, M. Cossi, N. Rega, J. M. Millam, M. Klene, J. E. Knox, J. B. Cross, V. Bakken, C. Adamo, J. Jaramillo, R. Gomperts, R. E. Stratmann, O. Yazyev, A. J. Austin, R. Cammi, C. Pomelli, J. W. Ochterski, R. L. Martin, K. Morokuma, V. G. Zakrzewski, G. A. Voth, P. Salvador, J. J. Dannenberg, S. Dapprich, A. D. Daniels, O. Farkas, J. B. Foresman, J. V. Ortiz, J. Cioslowski, D. J. Fox, Gaussian, Inc., Wallingford CT, **2010**.

[36] A. D. Becke, *J. Chem. Phys.* **1993**, *98*, 5648–5652.

[37] C. Lee, W. Yang, R. G. Parr, *Phys. Rev. B* **1988**, *37*, 785–789.

[38] P. J. Stephens, F. J. Devlin, C. F. Chabalowski, M. J. Frisch, *J. Phys. Chem.* **1994**, *98*, 11623–11627.

[39] a) G. A. Petersson, M. A. Al-Laham, *J. Chem. Phys.* **1991**, *94*, 6081–6090; b) G. A. Petersson, A. Bennett, T. G. Tensfeldt, M. A. Al-Laham, W. A. Shirley, J. Mantzaris, *J. Chem. Phys.* **1988**, *89*, 2193–2218.

[40] T. Yanai, D. P. Tew, N. C. Handy, *Chem. Phys. Lett.* **2004**, *393*, 51–57.

[41] a) S. Jungsuttiwong, V. Tarsang, T. Sudvoadsuk, V. Promarak, P. Khongpracha, S. Namuangruk, *Org. Electron.* **2013**, *14*, 711–722; b) J. Preat, *J. Phys. Chem. C* **2010**, *114*, 16716–16725; c) P. Wiggins, J. A. G. Williams, D. J. Tozer, *J. Chem. Phys.* **2009**, *131*, 091101 (1–4); d) M. J. G. Peach, A. J. Cohen, D. J. Tozer, *Phys. Chem. Chem. Phys.* **2006**, *8* 4543–4549; e) M. J. G. Peach, T. Helgaker, P. Sałek, T. W. Keal, O. B. Lutnæs, D. J. Tozer, N. C. Handy, *Phys. Chem. Chem. Phys.* **2006**, *8* 558–562; f) M. J. G. Peach, P. Benfield, T. Helgaker, D. J. Tozer, *J. Chem. Phys.* **2008**, *128*, 044118(1–8).

[42] a) W. Li, C. Du, F. Li, Y. Zhou, M. Fahlman, Z. Bo, F. Zhang, *Chem. Mater.* **2009**, *21*, 5327–5334; b) S. Fuse, H. Yoshida, T. Takahashi, *Tetrahedron Lett.* **2012**, *53*, 3288–3291; c) A. Leliège, P. Blanchard, T. Rousseau, J. Roncali, *Org. Lett.* **2011**, *13*, 3098–3101.

Received: ((will be filled in by the editorial staff))
Revised: ((will be filled in by the editorial staff))
Published online: ((will be filled in by the editorial staff))

DOI: 10.1002/chem.201xxxxxx

Entry for the Table of Contents (Please choose one layout only)

Layout 1:

FULL PAPER

D-π-A organoboron compounds with tunable push-pull character have been prepared by varying the donor and acceptor groups. Efficient green to NIR emission has been achieved from these compounds in solution. Aggregation-induced emission was observed for one compound. Each compound showed a strong and clearly visible response to fluoride addition, with either a large emission-color change or turn-on fluorescence.

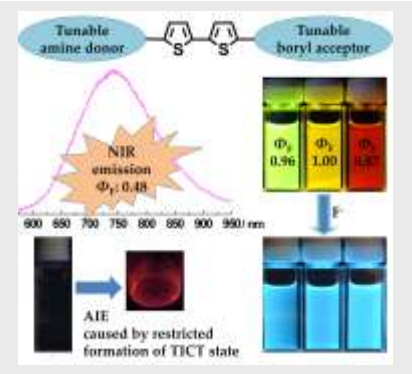

Fluorescence

*Zuolun Zhang, Robert M. Edkins, Jörn Nitsch, Katharina Fucke, Antonius Eichhorn, Andreas Steffen, Yue Wang, and Todd B. Marder**

■■ – ■■

D-π-A Triarylboron Compounds with Tunable Push-Pull Character Achieved by Modification of Both the Donor and Acceptor Moieties